catalysts

MDPI

Review

Recent Advances on Furan-Based Visible Light Photoinitiators of Polymerization

Frédéric Dumur

Aix Marseille University, CNRS, ICR, UMR 7273, F-13397 Marseille, France; frederic.dumur@univ-amu.fr

Abstract: Photopolymerization is an active research field enabling to polymerize in greener conditions than that performed with traditional thermal polymerization. At present, a great deal of effort is devoted to developing visible light photoinitiating systems. Indeed, the traditional UV photoinitiating systems are currently the focus of numerous safety concerns so alternatives to UV light are being actively researched. However, visible light photons are less energetic than UV photons so the reactivity of the photoinitiating systems should be improved to address this issue. In this field, furane constitutes an interesting candidate for the design of photocatalysts of polymerization due to its low cost and its easy chemical modification. In this review, an overview concerning the design of furane-based photoinitiators is provided. Comparisons with reference systems are also established to demonstrate evidence of the interest of these photoinitiators in innovative structures.

Keywords: furane; photocatalyst; visible light; photopolymerization; type II photoinitiators; oxime esters; free radical polymerization

check for updates

Citation: Dumur, F. Recent Advances on Furan-Based Visible Light Photoinitiators of Polymerization. *Catalysts* **2023**, *13*, 493. https://doi.org/10.3390/catal13030493

Academic Editors: Detlef W. Bahnemann and Jorge Bedia

Received: 11 February 2023
Revised: 26 February 2023
Accepted: 27 February 2023
Published: 28 February 2023

1. Introduction

During the past decade, major efforts have been devoted to developing polymerization processes more respectful of the environment [1–16]. In this field, photopolymerization offers several advantages compared to the traditional solution-phase polymerization. As an interesting feature, photopolymerization can be carried out without solvents, to obtain temporal and spatial control of the polymerization process but also to polymerize in energy-saving conditions [17–30]. Indeed, light-emitting diodes (LEDs) have become popular light sources that are now unavoidable in photopolymerization [31–35]. Contrary to UV irradiation setups that are energy-consuming and expensive, LEDs are cheap, compact, lightweight, long-living, and energy-saving devices. LEDs also offer the possibility to polymerize under visible light, which constitutes a major advantage in terms of light penetration within the photocurable resin but also in terms of safety for the manipulator [36–39]. Production of ozone during polymerization can also be avoided if visible light sources are used [39]. Indeed, a light penetration ranging between a few millimeters at 400 nm and around 5 cm at 800 nm can be obtained in the visible range whereas the light penetration remains limited to a few hundreds of micrometers if UV light is used [40]. As a drawback to this improved light penetration, visible light photons are also less energetic than UV photons so this issue can only be overcome by developing photoinitiating systems of higher reactivity. Intense research activity on photopolymerization is notably supported by the numerous applications making use of photopolymerization. Among the most popular applications, dentistry, 3D and 4D printing, solvent-free paints, adhesives, coatings, microelectronics, and varnishes can be cited as relevant examples [1–10]. With regard to the reactivity of the photoinitiating systems, numerous structures have been examined over the years. Among them, naphthalimides [41–59], pyrenes [60–68], benzophenones [69–76], carbazoles [77–90], thioxanthones [29,91–103], camphorquinone [104,105], curcumin [106–109], dihydroanthraquinones [110], silyl glyoximides [111], iodonium salts [41,112–118], *N*-heterocyclic carbene boranes [30], phenothiazines [119–129], copper complexes [130–134],

iridium complexes [135–139], benzoyl formates and related derivatives [140–142] or chalcones [9,143–156] are among the most widely studied structures of the last few years. Investigation of these different photoinitiating systems notably enabled the identification of highly reactive structures. Photoinitiating systems that can efficiently promote polymerization under sunlight [157–166] or in water [23,103,152,167–181] are also actively researched as these systems certainly constitute the photoinitiating systems of tomorrow. In fact, photoinitiators can be divided into two distinct categories differing in how the initiating radicals are produced. Thus, Type I photoinitiators consist of dyes capable to undergo, upon excitation, a homolytic "α-cleavage" to produce free-radical species (See Scheme 1) [182–191]. In this field, benzoin ether derivatives, benzyl ketals, acylphosphine oxides, acetophenones, aminoalkyl phenones, *O*-acyl-α-oximino ketones, acylgermanes, α-hydroxyalkyl ketones, hydroxylalkylphenones, α-aminoketones, and oxime esters have been extensively studied [192]. Type I photoinitiators are typically monocomponent systems and do not require any additives to produce radicals. As a drawback, during the polymerization process, an irreversible consumption of the photoinitiator occurs. Conversely, Type II photoinitiators are bimolecular photoinitiators that can lead, in the presence of a hydrogen donor, to the formation of a ketyl radical and a second radical derived from the hydrogen donor molecule [92,97,193–198]. In order to introduce the photosensitizer in a catalytic amount, a sacrificial amine is often used. Considering that most of the photoinitiating systems are three-component systems in order to exhibit sufficient reactivity, the complexity of the formulation is often evoked as a drawback of this strategy. Type II photoinitiators are often combined with onium salts which can generate initiating radicals subsequent to the photoinduced electron transfer between the photosensitizer and the onium salt (See Scheme 1) [199–204]. As an advantage of this approach, the photosensitizer can be introduced in a catalytic amount, with the sacrificial amine acting as a reductant capable to regenerate the photoinitiator in its initial redox state during the polymerization process.

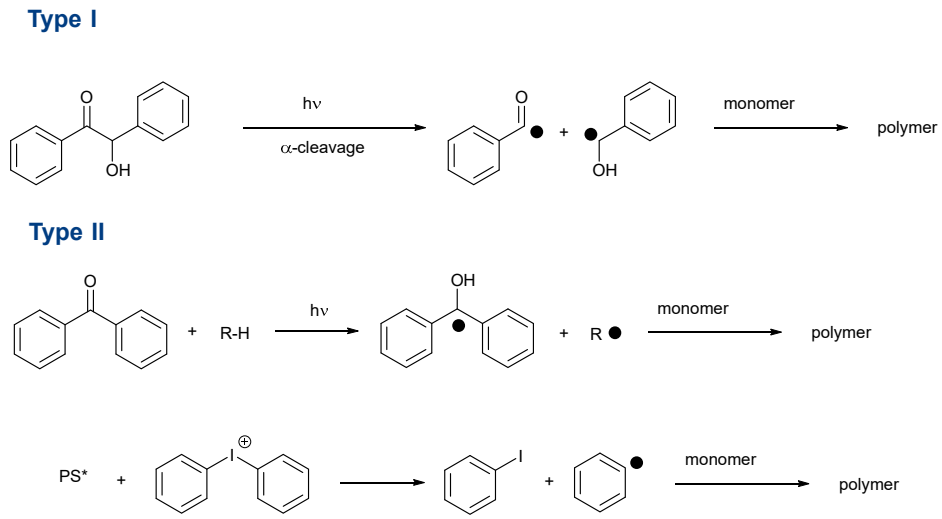

Scheme 1. Radical generation with Type I and Type II photoinitiators (* corresponds to the excited dye).

Among structures that can be used for the design of photoinitiators or photosensitizers, furane has only been used scarcely, contrary to thiophene which was a popular building block [91,126,205–210]. Furan is a heterocyclic five-membered ring that is extensively used for the design of anti-inflammatory and antimicrobial agents [211]. Furan was also used for the design of semi-conducting materials for organic solar cells [212] and field effect transistors [213, 214], the design of fluorescent materials [215] and light-emitting materials [216,217] or host materials [218] for organic light-emitting diodes. Furan exhibits a low toxicity, even if recent reports have demonstrated that furan can be formed during the thermal treatment of food and

can be carcinogenic [219]. Notably, furan can facilely accumulate in the liver [220]. However, due to its interesting redox potential, and its good thermal and photochemical stability, furane remains a candidate of choice for designing photoinitiators. In this review, an overview of the recent advances concerning the design of visible light photoinitiating systems comprising furane is provided. Parallel to the description of the different structures and with the aim of evidencing the pertinence of this approach, a comparison with reference systems composed of benchmark photoinitiators is provided.

2. Furane-Based Photoinitiators of Polymerization

2.1. Benzylidene Ketones

The first report mentioning the use of a furane-based benzylidene ketone (BFC) as a photoinitiator of polymerization was reported in 2019 by Nie and coworkers (See Figure 1) [221]. 2,6-*Bis*(furan-2-ylmethylidene)cyclohexan-1-one (BFC) could be prepared in one step, by condensation of furfural with cyclohexanone in quantitative yield. Based on its absorption extending between 300 and 450 nm with an absorption maximum located at 373 nm, this dye was thus appropriate for photopolymerization experiments carried out at 365, 385, and 405 nm (See Figure 2).

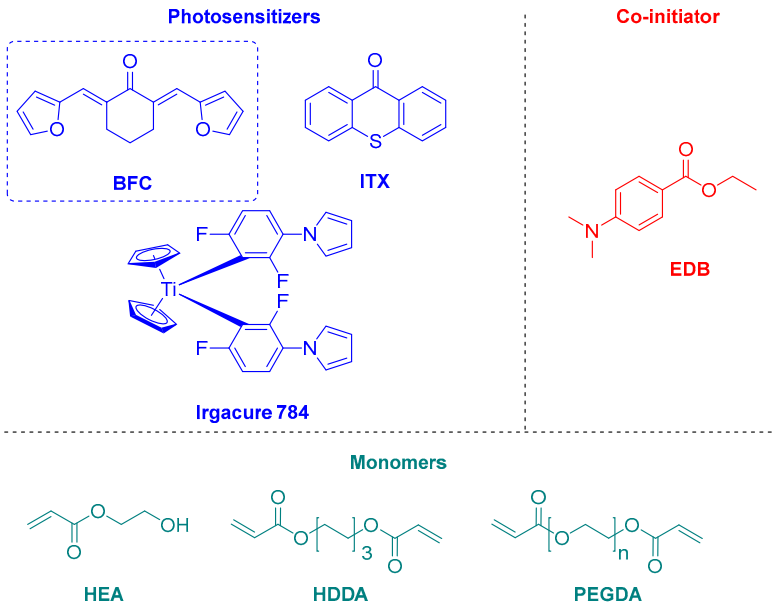

Figure 1. Chemical structures of BFC and different additives.

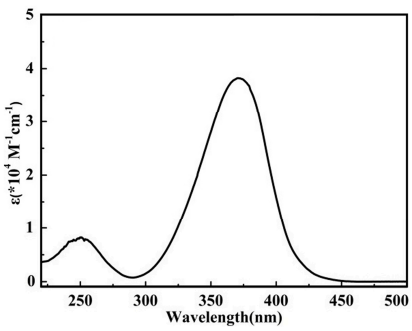

Figure 2. UV-visible absorption spectrum of BFC in acetonitrile. Reproduced with permission of Ref. [221].

Interestingly, BFC could initiate the free radical polymerization (FRP) of hexamethylene diacrylate (HDDA) and polyethylene glycol diacrylate (PEGDA) upon irradiation at

365 nm with a LED (light intensity: 70 mW/cm^2) without any additives. At similar concentrations, higher monomer conversions could be obtained for PEGDA compared to HDDA. Thus, if a conversion of 70% in 900 s could be determined for PEGDA, this value decreased to only 30% for HDDA. The best monomer conversions were obtained at very low photoinitiator content, namely 0.0625 wt%. BFC can thus be used in a catalytic amount. At 405 nm, a different situation was found since the HDDA conversion decreased to only 10% whereas that of PEGDA increased up to 80%. It was thus concluded that PEGDA was acting as a co-initiator for BFC. Noticeably, the addition of 5 wt% of ethyl 4-dimethylaminobenzoate (EDB) in HDDA did not contribute to drastically improving the HDDA conversion whereas the addition of 5 wt% of PEGDA in HDDA increased the HDDA conversion up to 60% upon irradiation at 405 nm for 900 s. This trend was confirmed during the FRP of hydroxyethyl acrylate (HEA), with the addition of PEGDA improving the monomer conversion. Comparison with the reference system based on 2-isopropylthioxanthone (ITX) revealed BFC to outperform ITX, irrespective of the polymerization conditions (See Figure 3).

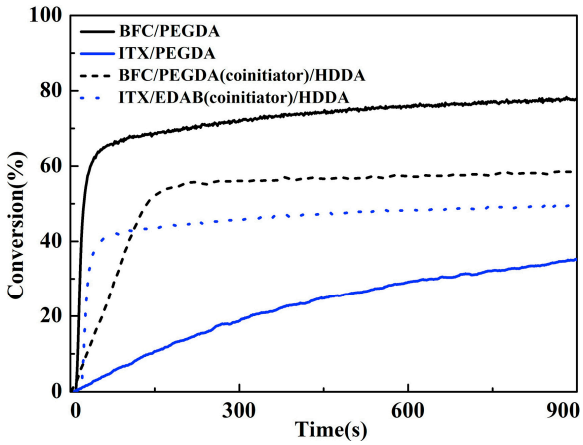

Figure 3. Monomer conversions obtained with ITX and BFC using different photoinitiating systems: BFC (0.0625 wt%)/PEGDA, ITX (0.0625 wt%)/PEGDA, BFC (0.0625 wt%)/PEGDA (5 wt%)/HDDA, ITX (0.0625 wt%)/EDAB (5 wt%)/HDDA upon irradiation with a LED emitting at 405 nm, 70 mW/cm^2. Reproduced with permission of Ref. [221].

To support the high monomer conversion obtained with PEGDA and on the basis of UV-visible absorption experiments, the authors suggested the formation of an exciplex between the monomer and BFC. Notably, a redshift of the absorption maximum for BFC from 373 nm in HDDA up to 389 nm in PEGDA, together with a broadening of the absorption spectrum up to 500 nm could be demonstrated. Overall, the mechanism depicted in Scheme 2 was proposed by the authors. Subsequent to the formation of the exciplex between BFC and PEGDA, and upon irradiation, the complex is promoted in its excited state so that a photoinduced electron transfer between PEGDA and BFC can occur. By proton transfer, initiating radicals can be formed. Parallel to this, efficient photobleaching of the resin could be observed during the polymerization process, resulting from the formation of ketyl radicals, suppressing the electron acceptor in BFC, and contributing to the discoloration of the final coating. Photobleaching properties of photoinitiators are highly researched, considering that visible light photoinitiators are strongly colored compounds that often impose color on the final coatings [88,108,120,140,191,221–233]. The photobleaching ability of BFC was also demonstrated during the 3D printing experiments performed using PEDGA as the monomer. For comparison, a benchmark photoinitiator absorbing in the same range was used, namely *bis*(2,6-difluoro-3-(1-hydropyrrol-1-yl)phenyl)titanocene (Irgacure 784). As shown in Figure 4, if the final printed object was strongly colored with Irgacure 784, a colorless object could be obtained with BFC.

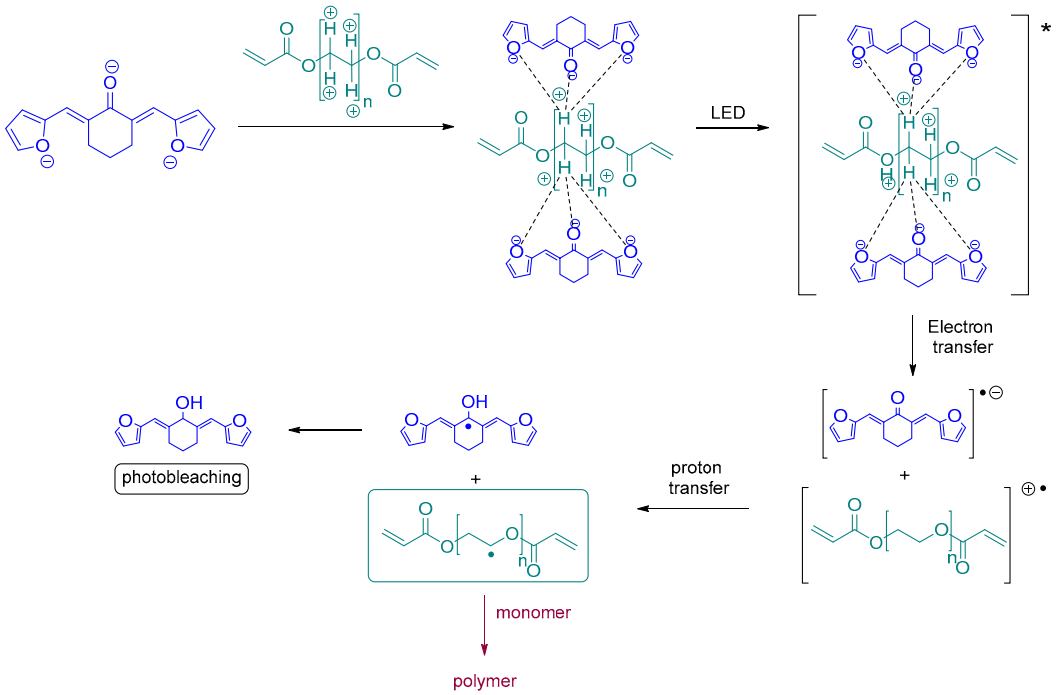

Scheme 2. Mechanism of photoinitiation and photobleaching with the BFC/PEGDA combination. (* corresponds to the excited dye).

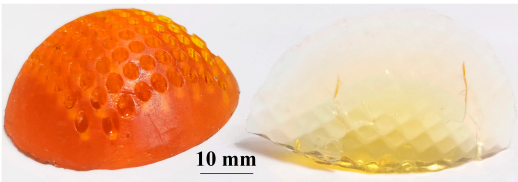

Figure 4. 3D-printed objects prepared with Irgacure 784 (**left**) and BFC (**right**). Reproduced with permission of Ref. [221].

Following this initial work, further investigations carried out by the same authors on BFC revealed the low photoinitiating ability of the BFC/EDB combination to originate from a rotation of the two peripheral furyl groups towards the central ketone group, adversely affecting the hydrogen transfer interaction with EDB [195]. Conversely, due to the strong interaction of BFC with PEGDA, molecular motion of the furyl groups is efficiently impeded, facilitating the hydrogen transfer interaction.

One year later, Lalevée and coworkers developed a series of benzylidene ketones still bearing furyl groups as peripheral groups (Ketone 1 and Ketone 3) but comprising different central groups. For comparison, an analog series was prepared, with peripheral thiophenes (ketone 4 and ketone 6) (See Figure 5) [234]. In this work, the FRP of acrylates and also the cationic polymerization (CP) of epoxides were investigated at 405 nm. Noticeably, modification of the central part in ketone 1-ketone 6 only slightly affected the position of the absorption maxima since a variation of only 5 nm could be found between the different dyes (See Table 1 and Figure 6). By replacing the furane group with a thiophene group, almost no modification of the absorption maxima was found, evidencing that the electron-donating ability of furane was comparable to that of thiophene. Besides, the highest molar extinction coefficients were determined for ketone 3 and ketone 4 bearing the central *N*-ethylpiperidinone. Based on their absorptions, photopolymerization experiments could be carried out at 405 nm with all dyes, in thin films, and in thick films.

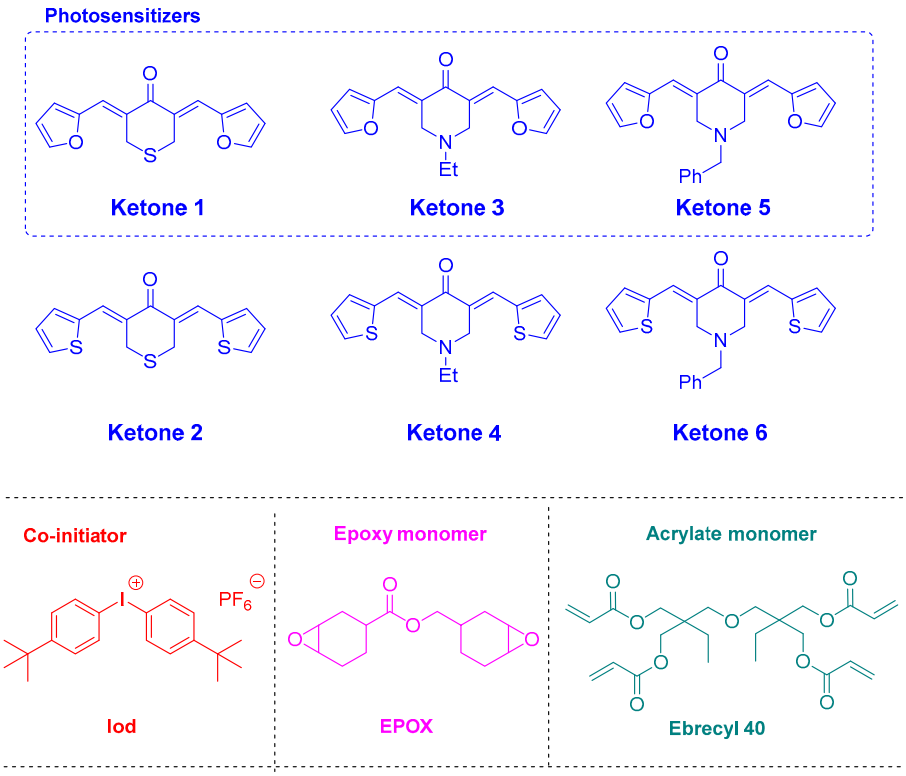

Figure 5. Chemical structures of ketones 1–6, different monomers and additives.

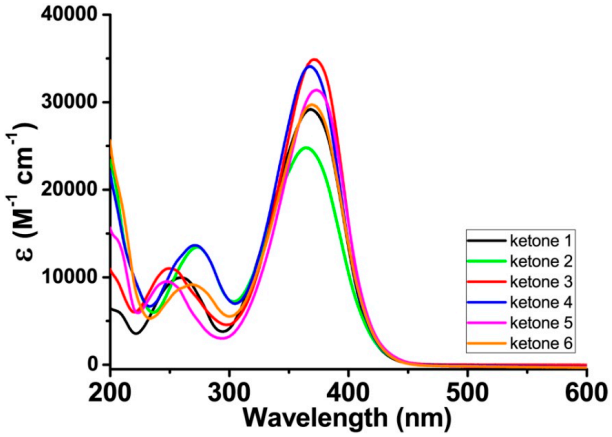

Figure 6. UV-visible absorption spectra of ketones 1–6 in acetonitrile. Reproduced permission from Ref. [234].

Table 1. Optical characteristics of ketones 1–6 in acetonitrile. Data extracted from Ref. [234].

	λ_{max} (nm)	ε_{max} ($M^{-1}.cm^{-1}$)	$\varepsilon_{@405\ nm}$ ($M^{-1}.cm^{-1}$)
ketone 1	368	29,230	9740
ketone 2	365	25,020	7980
ketone 3	370	34,920	11,690
ketone 4	368	34,200	10,130
ketone 5	372	31,470	11,950
ketone 6	370	29,750	10,280

Despite the similarity of their absorptions, major differences could be found between the different dyes in terms of monomer conversions. For the different experiments, three-component benzylidene ketones/amine/Iod (0.1%/2%/2%, *w*/*w*/*w*) systems were used.

Here again, after optimization of the polymerization conditions, a very low photoinitiator content could be used. Thus, in thick films, the best monomer conversion was obtained with ketone 3, peaking at 94% after 400 s of irradiation at 405 nm. For comparison, its thiophene analog i.e., ketone 4 only furnished a conversion of 24% (See Table 2). The benefits of introducing a furane group in benzylidene ketones were thus demonstrated. A slight reduction of the monomer conversion was observed with the more sterically hindered ketone 5, reaching 90%. In the case of ketone 1 and ketone 2 comprising a central thiopyranone, only low monomer conversions were obtained, below 30%. In thin films, an inversion of reactivity between ketone 3 and ketone 4 was found, with ketone 4 outperforming ketone 3 (81% vs. 55% conversion for ketone 3). It therefore clearly evidenced the crucial role of the substitution pattern of benzylidene ketones on the reactivity, but also the necessity to test all dyes in thin and in thick films. Steady-state photolysis experiments performed in solution for ketone 3 revealed this dye to interact both with Iod and EDB in oxidative and reductive pathways. Besides, faster photolysis was evidenced with Iod than with EDB (See Figure 7).

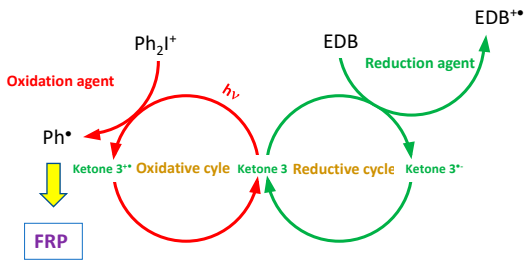

Figure 7. Photochemical mechanism occurring with ketone 3 used as a photosensitizer.

Table 2. Final conversions obtained for Ebecryl 40 in thick and thin films using the three-component benzylidene ketones/amine/Iod (0.1%/2%/2%, *w*/*w*/*w*) system, irradiation at 405 nm with a LED for 400 s. Data extracted from Ref. [234].

	Ketone 1	Ketone 2	Ketone 3	Ketone 4	Ketone 5	Ketone 6
FCs (thick films)	30%	24%	94%	24%	90%	25%
FCs (thin films)	55%	67%	55%	81%	59%	71%

Due to the high reactivity of ketone 3 during the FRP of Ebecryl 40, the cationic polymerization of (3,4-epoxycyclohexane)methyl 3,4-epoxycyclohexylcarboxylate (EPOX) was also investigated with the two-component ketone 3/Iod (0.1%/2%, *w*/*w*) system. After 400 s of irradiation, a final monomer conversion of 50% could be determined, making ketone 3 a photoinitiator as efficient in FRP as in CP.

Following this work, the same authors investigated the reactivity of the extended version of ketone 3, namely ketone 3′ in the same conditions as ketone 3 (See Figure 8) [146]. Due to the extended π-conjugation in ketone 3′, a redshift of the absorption maximum to 405 nm was determined for ketone 3′, with a slight increase of the molar extinction coefficient compared to ketone 3 (ε = 37,700 $M^{-1}.cm^{-1}$ vs. 34,920 $M^{-1}.cm^{-1}$ for ketone 3). Polymerization tests revealed ketone 3′ to furnish a higher monomer conversion than ketone 3 in thin films (68% vs. 55% for ketone 3). Conversely, a lower conversion was obtained during the CP of EPOX with ketone 3′ compared to ketone 3 (27% vs. 50% for ketone 3). These differences in reactivity can be assigned to different molar extinction coefficients at 405 nm but also to different rate constants of the interaction of ketone 3 and ketone 3′ with the different additives. The introduction of a less flexible central part was also investigated, as exemplified with Dye 1 and Dye 9 [151].

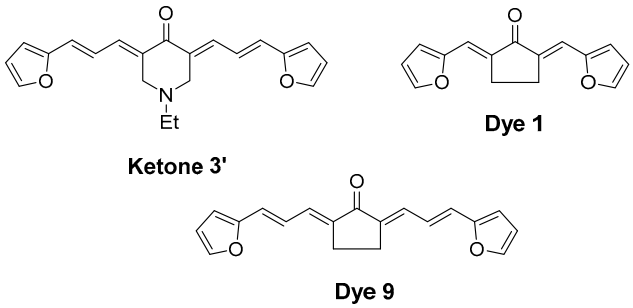

Figure 8. Chemical structures of ketone 3′, dye 1, and dye 9.

Here again, the higher reactivity of the more extended Dye 9 compared to Dye 1 was confirmed in thin films, at 405 nm but also at 470 nm during the FRP of PEGDA (See Table 3). It can tentatively be assigned to a reduction of the redox potentials for the extended dyes, enabling these structures to interact more efficiently with the iodonium salt.

Table 3. Final conversions obtained during the FRP of PEGDA in thick and thin films using the three-component benzylidene ketones/amine/Iod (0.1%/2%/2%, *w*/*w*/*w*) system, irradiation at 405 or 470 nm with a LED for 200 s. Data extracted from Ref. [151].

	LED@405 nm		LED@470 nm	
	Dye 1	**Dye 9**	**Dye 1**	**Dye 9**
FCs (thick films)	7%	14%	-	-
FCs (thin films)	76%	90%	40%	63%

2.2. Charge Transfer Complexes Based on Benzylidene Ketones

The design of water-soluble photoinitiators is an active research field as it paves the way toward photopolymerization in water. If the chemical modification of well-known photoinitiators constitute hard work in order to render the dyes water-soluble, recently, an interesting approach was proposed. This involves minimizing the synthetic step to a simple mixture of the targeted photoinitiator with a water-soluble amine in order to prepare water-soluble charge transfer complexes (CTC). Using this approach, no chemical modification of the organosoluble photoinitiator is required [235–249]. This approach, if recently revisited in the context of photopolymerization, is not new since one of the first reports mentioning the use of water-soluble charge transfer complexes in photopolymerization was published as early as 1973 by Shigeho Tazuke [250]. In recent chemistry, triethanolamine (TEOA) is among the most widely used water-soluble amines due to its remarkable water-solubility and its easy availability. In 2020, 2,6-*bis*(furan-2-ylmethylidene)cyclohexan-1-one (BFC) was revisited by Nie and coworkers in the context of the design of water-soluble photoinitiators [167]. As anticipated, the formation of a CTC between TEOA and BFC resulted in a redshift of the absorption maxima from 373 nm for BFC up to 400 nm for $[BFC/TEOA]_{CTC}$ in acetonitrile (See Figures 9 and 10).

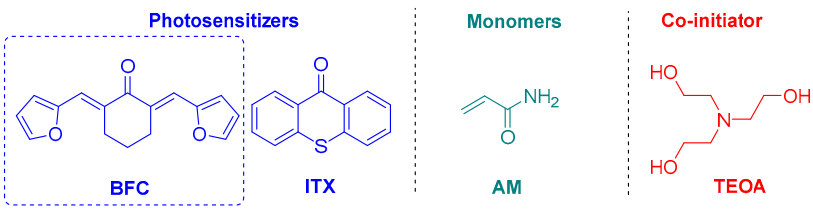

Figure 9. Chemical structures of BFC, ITX, AM, and TEOA.

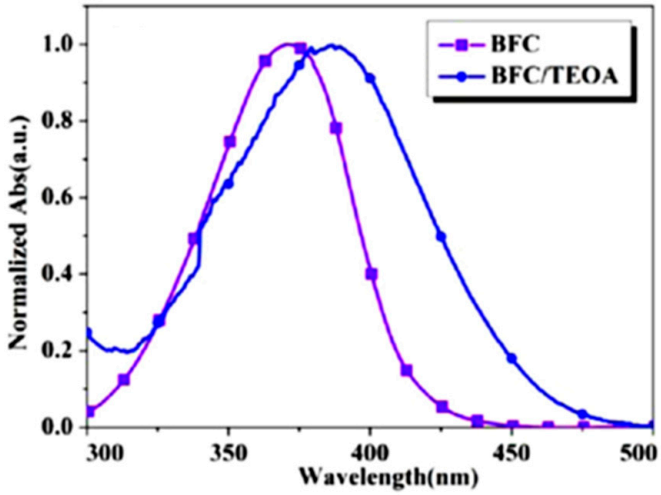

Figure 10. UV-visible absorption spectra of BFC and $[BFC/TEOA]_{CTC}$. Reproduced with permission of Ref. [167].

The CTC exhibited good solubility in water since a saturation concentration of 20 mg/mL was determined. At 3 wt% CTC in water, the polymerization efficiency of acrylamide (AM) reached an optimum, and a final monomer conversion higher than 80% could be determined after 900 s of irradiation at 405 nm (I = 70 mW/cm^2) (See Figures 10 and 11) Monomer conversions were obtained during the FRP of acrylamide upon irradiation at 405 nm (70 mW/cm^2) using the $[BFC/TEOA]_{CTC}$ as the photoinitiating system.

To support the polymerization process detected with the BFC/TEOA combination, the mechanism depicted in Figure 11 was proposed by the authors. Notably, upon excitation of the CTC, a photoinduced electron transfer between TEOA and BFC can occur. By hydrogen abstraction, ketyl radicals as well as α-amino alkyl radicals acting as initiating species can be formed.

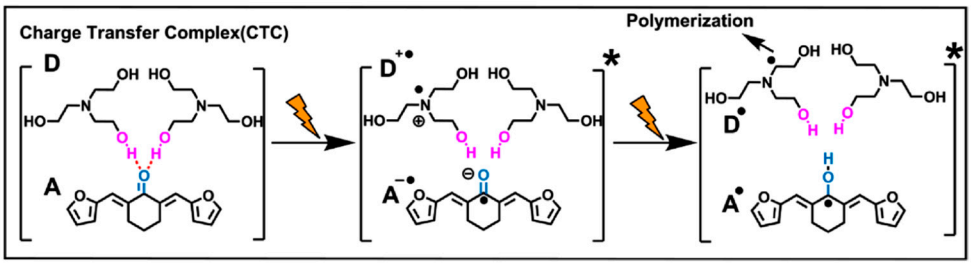

Figure 11. Mechanism involved in the polymerization process with the $[BFC/TEOA]_{CTC}$. Reproduced with permission of Ref. [167] (* corresponds to the excited state).

Finally, the existence of a CTC between BFC and TEAO was confirmed by theoretical calculations. As can be seen from Figure 12, the highest occupied molecular orbital (HOMO) of TEOA stands between the HOMO and the lowest unoccupied molecular orbital (LUMO) of BFC, supporting an electron transfer between TEOA and BFC. Concerning the $[BFC/TEOA]_{CTC}$, the location of the HOMO energy level on TEOA and the LUMO energy level on BFC could be clearly evidenced. A stabilization energy of 5.85 kcal/mol was determined by theoretical calculations, favorable to the formation of a CTC between TEOA and BFC.

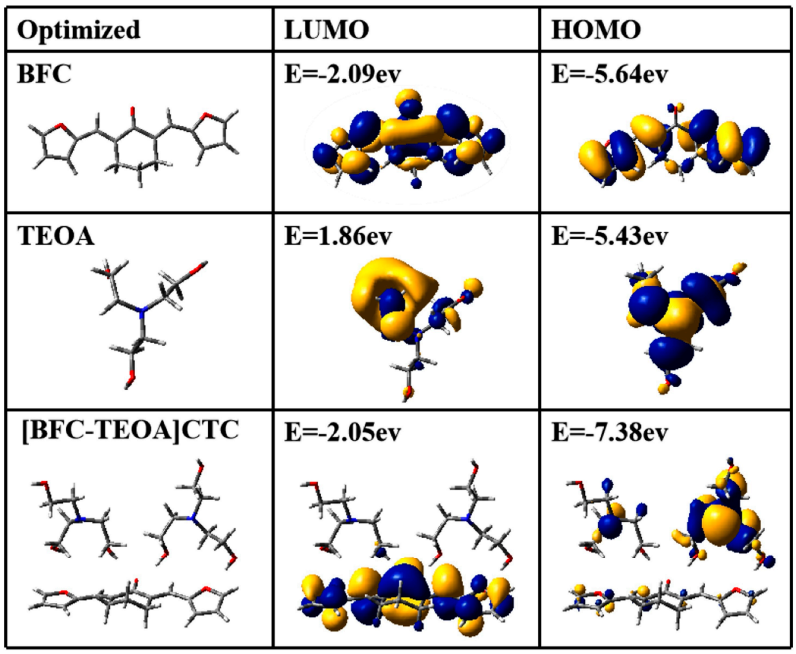

Figure 12. Contour plots of the HOMO and LUMO energy levels of BFC, TEOA, and $[BFC/TEOA]_{CTC}$. Reproduced with permission of Ref. [167].

2.3. Chalcones

Parallel to benzylidene ketones that are sometimes named *bis*-chalcones, chalcones have also recently been the focus of numerous studies as visible light photoinitiators of polymerization [150]. The interest in these structures relies on the fact that chalcones are bio-inspired structures that can be easily obtained by a Claisen Schmidt condensation of an aldehyde and an acetophenone in safe solvents such as ethanol and by using potassium or sodium hydroxide as the base. Additionally, chalcones often precipitate in alcohols so their purification is often reduced to a simple filtration and washing with water. Chalcones also exhibit biological activities such as antioxidant, antimicrobial, antifungal, antitumor, anticancer, antimalarial, anti-inflammatory, and antidepressant [251–255]. In 2020, a series of furane-based chalcones CHC-13-CHC-17 was proposed by Lalevée and coworkers (See Figure 13) [143]. Efficient monomer conversions could only be obtained while using a three-component chalcone/Iod/EDB (1.5%/1.5%/1.5% *w*/*w*/*w*) system, thus enabling the chalcone to be regenerated during the polymerization process.

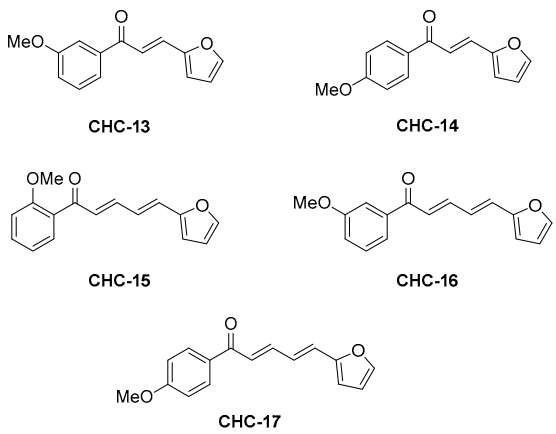

Figure 13. Chemical structures of CHC-13-CHC-17.

Using the three-component system, monomer conversions ranging between 65% for CHC-16 to 79% for CHC-15 were determined in thin films using PEGDA as the monomer and upon irradiation at 405 nm with a LED (See Table 4). Here again, the crucial influence of the substitution pattern was demonstrated. Indeed, CHC-15-CHC-17 only differs by the substitution pattern and the position of the methoxy group. Thus, the lowest monomer conversion was obtained for CHC-16 in which the methoxy group was in a non-conjugated position with regards to the ketone group of acetophenone. Compared to the monomer conversions obtained with the previously mentioned benzylidene ketones Dye 1 and Dye 9, chalcones CHC-13-CHC-17 proved to be less efficient photoinitiators since lower monomer conversions were obtained with these structures. Investigation of the photochemical mechanism revealed the chalcone/EDB combination to give faster photolysis than the chalcone/Iod combination. Therefore, the concomitant presence of an oxidative and a reductive cycle enabling to simultaneously generate different initiating species (Ph•, $EDB_{(-H)}$•, Dye-H•) could efficiently produce radicals (See Figure 14).

Table 4. Monomer conversions obtained during the FRP of PEGDA upon irradiation at 405 nm using the three-component Chalcone/Iod/EDB (1.5%/1.5%/1.5% *w*/*w*/*w*) photoinitiating systems in thin films. Data extracted from Ref. [143].

Chalcone	CHC-13	CHC-14	CHC-15	CHC-16	CHC-17
FCs	73%	74%	79%	65%	69%

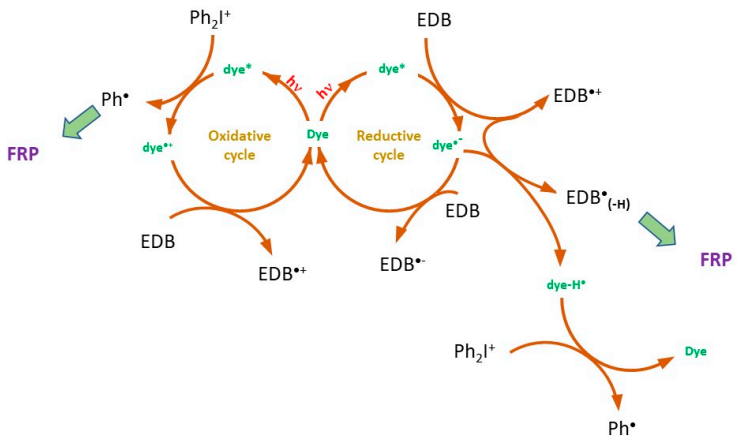

Figure 14. Photochemical mechanism occurring with the three-component chalcone/Iod/EDB system.

In the previous series CHC-13-CHC-17, furane was used as an electron-donating group. However, the furyl group can also be incorporated into the acetophenone side, which was performed with A5 (See Figure 15) [148]. In order to investigate the contribution of furane in this structure, a series of seven chalcones A1–A7 was prepared, all comprising anthracene as the electron-donating group. The only difference is the group introduced on the acetophenone side.

Logically, absorption maxima of A1–A7 were similar, the electronic delocalization being the same in these different structures. Indeed, the color of chalcones originates from the π-conjugation existing between the anthracenyl unit and the ketone group. In the present case, absorption maxima ranging between 387 nm for A4 and A6 up to 389 nm for A1, A5, and A7 were determined in acetonitrile (See Figure 16 and Table 5). For comparison, dibutoxyanthracene (DBA) [256] was used as a reference compound due to the similarity of its absorption with A1–A7.

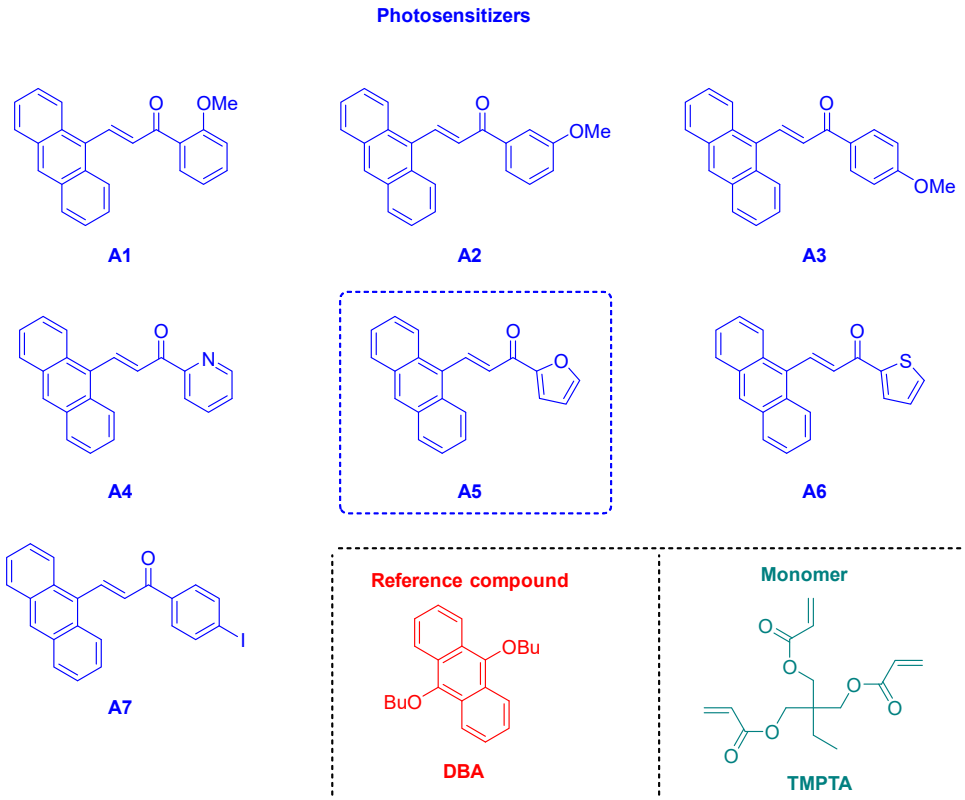

Figure 15. Chemical structures of A1–A7 and DBA.

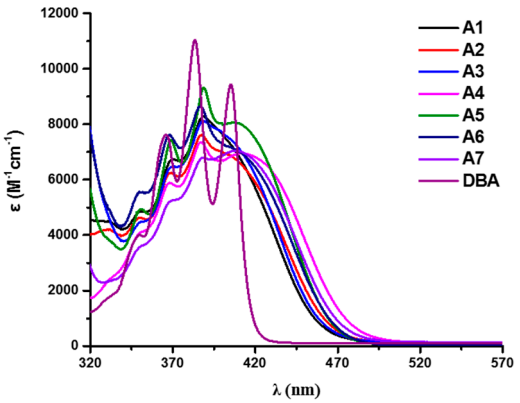

Figure 16. UV-visible absorption spectra of A1–A7 in acetonitrile. Reproduced with permission of Ref. [148].

Table 5. Optical characteristics of A1–A7 in acetonitrile. Data extracted from Ref. [148].

	λ_{max} (nm)	ε_{max} ($M^{-1}.cm^{-1}$)	ε405 nm ($M^{-1}.cm^{-1}$)	ε470 nm ($M^{-1}.cm^{-1}$)
A1	389	8300	7300	400
A2	388	7600	6900	550
A3	388	8100	7400	450
A4	387	7300	6800	1350
A5	389	9300	8000	600
A6	387	8700	7200	650
A7	389	6800	7000	900
DBA	384	11,000	9400	0

Theoretical calculations performed on A5 revealed the HOMO energy level to be located on the anthracene moiety whereas the LUMO energy level is clearly centered on the acetophenone moiety, consistent with the push-pull structures and the electronic delocalization existing in chalcones (See Figure 17).

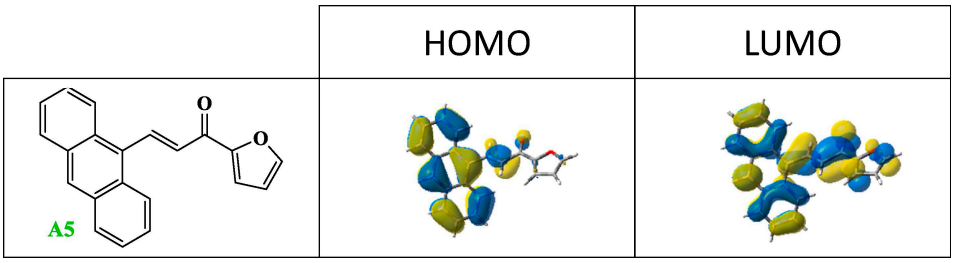

Figure 17. Contour plots of the HOMO and LUMO energy levels of A5. Reproduced with permission of Ref. [148].

Examination of their photoinitiating ability in three-component chalcone/Iod/EDB (0.5%/1%/1%, *w*/*w*/*w*) systems revealed A4, A5, and A6 to furnish the highest final monomer conversions during the FRP of trimethylolpropane triacrylate (TMPTA) (See Table 6). Interestingly, conversions obtained with A5 were comparable to that of A6, evidencing that the five-membered ring furane and thiophene derivatives could furnish dyes of similar reactivity. Blank experiments performed with the Iod/EDB combination only furnished a monomer conversion of 5%, evidencing the crucial role of the dye in the light absorption mechanism. While using the two-component chalcone/Iod (0.5%/1%, *w*/*w*) system, A5 could also furnish a high EPOX conversion under air. If a monomer conversion of 52% was obtained at 405 nm, this value decreased to 36% at 470 nm, consistent with a reduction of the molar extinction coefficient of A5 at this wavelength. For comparison, the benchmark photoinitiating system DBA/Iod only furnished a conversion of 38%, far behind that of A5. Interestingly, photolysis experiments performed in solution revealed the two-component A5/Iod and A5/EDB systems to give similar photolysis rates, supporting the high efficiency in photopolymerization by the concomitant occurrence of the oxidative and reductive pathways contributing to the efficient generation of initiating radicals. Based on the high reactivity of the furane-based chalcone A5, 3D printing experiments could be carried out and 3D patterns exhibiting an excellent spatial resolution could be prepared (See Figure 18).

Table 6. TMPTA and EPOX conversions obtained with the three-component chalcone/Iod/EDB (0.5%/1%/1%, *w*/*w*/*w*) systems upon irradiation at 405 nm in thin films. Data extracted from Ref. [148].

PIS	TMPTA (%)	EPOX (%)	
	Dyes/Iod/EDB [a]	Dyes/Iod [a]	Dyes/Iod [b]
A1	57	39	21
A2	51	37	24
A3	45	21	15
A4	60	43	33
A5	60	52	36
A6	61	47	27
A7	45	33	19
Blank [c]	5	-	-
DBA	-	38	6

[a] Upon irradiation at 405 nm. [b] upon irradiation at 470 nm. [c] Iod/EDB (1%/1% *w*/*w*).

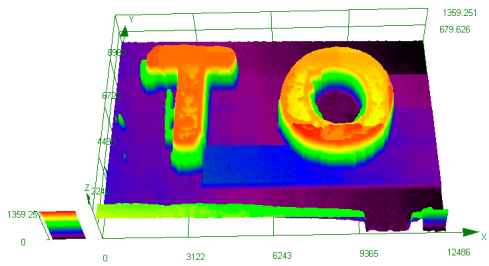

Figure 18. 3D printing experiments performed using EPOX as the monomer, upon irradiation at 405 nm and by using the two-component A5/Iod (0.5%/1%, *w*/*w*) system. Reproduced with permission of Ref. [148].

2.4. Coumarins

In all the above-mentioned examples, furane-based compounds have been used as Type II photoinitiators, meaning that the different dyes can only produce initiating radicals in multi-component systems. Conversely, Type I photoinitiators are mono-component systems and in this field, oxime esters are popular photoinitiators due to their low cost, easiness of synthesis, and good thermal stability [182–191]. Type I photoinitiators certainly constitute the photoinitiators of tomorrow as no additional additives are required to generate initiating species. A drastic simplification of the photocurable resin can thus be obtained. In 2020, Dietliker and coworkers examined a series of coumarin-based oxime esters varying by the photocleavable group (See Figure 19) [191]. Indeed, from the mechanistic viewpoint, upon photoexcitation, the homolytic cleavage of the N-O bond can occur, producing iminyl and aryloxy radicals. Subsequent to fragmentation, the aryloxy radicals can undergo a decarboxylation reaction, generating aryl radicals (See Scheme 3). The release of carbon dioxide within the resin during the polymerization is an important parameter as it can contribute to limiting oxygen diffusion within the resin by the release of a gas inside the resin. Carbon dioxide release is not limited to oxime esters and phenyl glyoxylates exhibit the same property [237,257–261]. On the basis of the photochemical mechanism, the decomposition of oxime esters is irreversible so that oxime esters cannot be introduced in a catalytic amount in the resins.

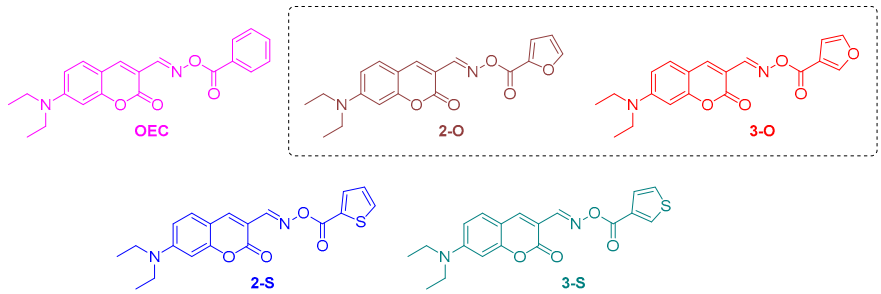

Figure 19. Chemical structures of coumarin-based oxime esters investigated by Dietliker and coworkers [191].

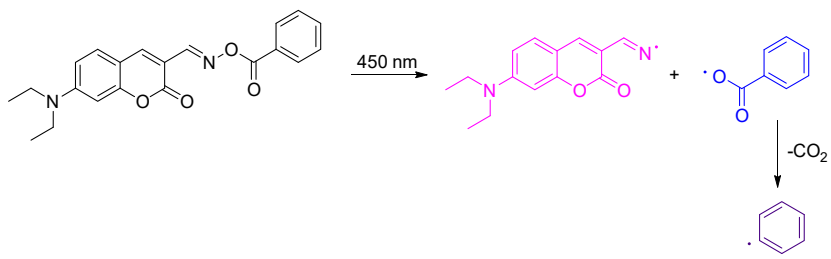

Scheme 3. Mechanism of photocleavage occurring from oxime esters and exemplified for OEC.

Considering that the chromophore is located in the coumarin moiety, the five coumarins exhibited similar absorption maxima, located at 436 nm (See Figure 20).

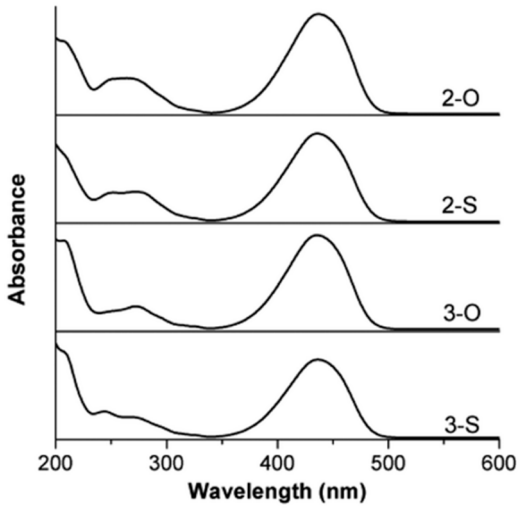

Figure 20. UV-visible absorption of 2-O, 2-S, 3-O, and 3-S at room temperature. Reproduced with permission of Ref. [191].

Photoinitiating abilities of the different dyes were investigated at 450 nm and the tetra-functional monomer TMPTA was selected for this study. Upon irradiation at 450 nm, the thiophenyl derivatives (2-S and 3-S) greatly outperformed the furanyl-based oxime esters (2-O and 3-O) (See Figure 21). Comparison between 2-O, 3-O, 2-S, and 3-S evidenced the 2-substituted heterocycles to outperform the 3-substituted heterocycles in terms of final monomer conversions. Comparison with OEC used as a reference oxime ester revealed all newly developed oxime esters to furnish lower monomer conversions than OEC. In fact, only the thiophene derivative 2-S could furnish monomer conversions approaching that of OEC.

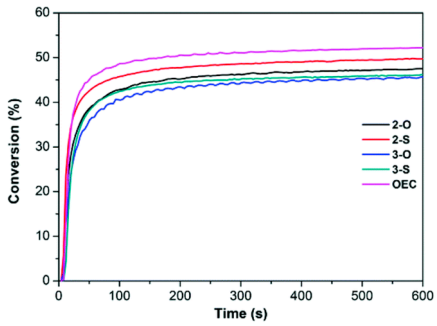

Figure 21. Monomer conversions obtained during the FRP of TMPTA using different oxime esters, irradiation at 450 nm with a LED (30 mW/cm^2). Reproduced with permission of Ref. [191].

With these considerations, comparisons were also established between 2-S and two benchmark photoinitiators, namely phenylbis(2,4,6-trimethylbenzoyl)phosphine oxide (BAPO, Irgacure 819) and diphenyl(2,4,6-trimethylbenzoyl)phosphine oxide (TPO). Comparisons were established at two different wavelengths, namely 405 and 450 nm (See Figure 22). At 405 nm, if a TMPTA conversion of 46% was obtained with 2-S, this conversion was vastly lower than that of BAPO or TPO (around 60% after 300 s of irradiation). Upon irradiation at 450 nm, based on different molar extinction coefficients at this wavelength, 2-S furnished a monomer conversion intermediate between that of BAPO and TPO. Due to the lack of absorption of TPO at 450 nm, a prolonged induction period could be evidenced for TPO so that a conversion of only 38% could be obtained. Overall, 2-S proved to be a relatively efficient photoinitiator while considering the fact that BAPO can

simultaneously produce four radicals per molecule contrary to 2-S which is only capable of producing one. In light of this consideration, furan and thiophene-based oxime esters can thus be considered better photoinitiators than BAPO.

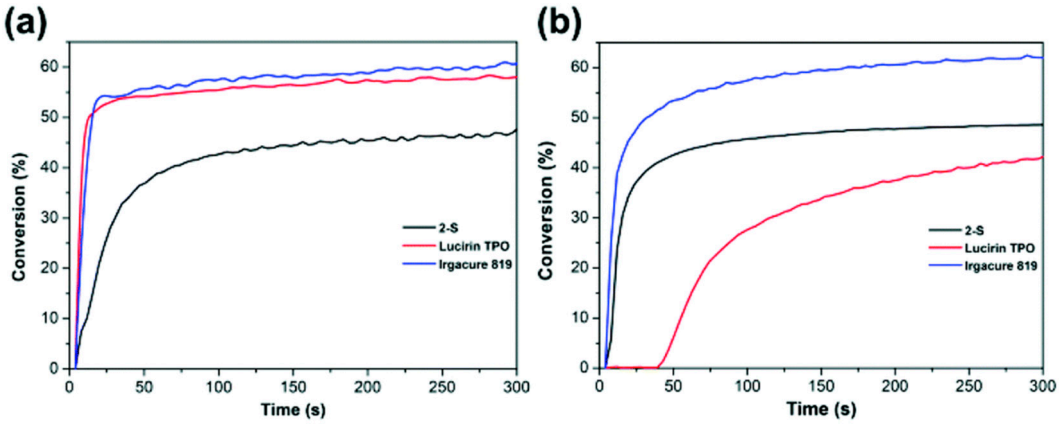

Figure 22. Polymerization profiles of TMPTA using 2-S, BAPO and TPO as photoinitiators (C = 2.7 × 10^{-5} mol.g^{-1} resin), upon irradiation at (**a**) 405 nm and (**b**) 450 nm with LEDs (I = 30 mW cm^{-2}). Reproduced with permission of Ref. [191].

Noticeably, 2-S exhibited interesting photobleaching properties in acetonitrile, with complete bleaching of the solution being detected within five min (See Figure 23). These photobleaching properties were confirmed during the thiol-ene polymerization of a TMPTA/PETMP blend (where PETMP stands for pentaerythritol tetra(3-mercaptopropionate). A complete bleaching of the polymer film could be obtained within one min. of irradiation at 450 nm. As a result of this fast photobleaching, polymer films as thick as 10 mm could be prepared within ten min. of irradiation at 450 nm.

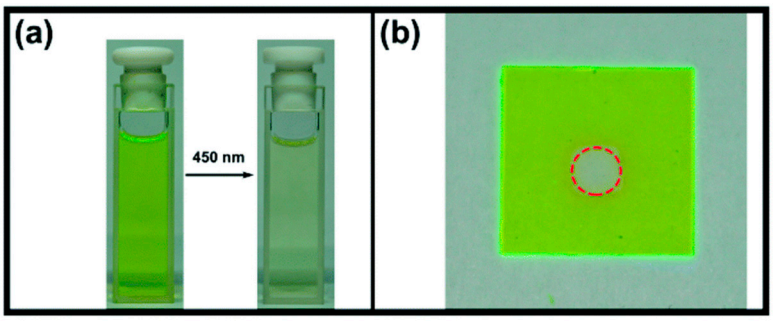

Figure 23. (**a**) Photolysis of 2-S (**a**) in acetonitrile, 450 nm irradiation (200 mW/cm^2). (**b**) Photobleaching during the thiol-ene polymerization of a TMPTA/PETMP blend. Reproduced with permission of Ref. [191].

Analysis of the thermal stability of the different oxime esters by thermogravimetric analyses revealed the decomposition temperatures to be higher than 160 °C, and thus sufficient for practical applications in industry.

3. Conclusions

To conclude, furane is an elemental building block that has been scarcely used up to now for the design of visible light photoinitiators. The different structures reported in this work are presented in Figure 24.

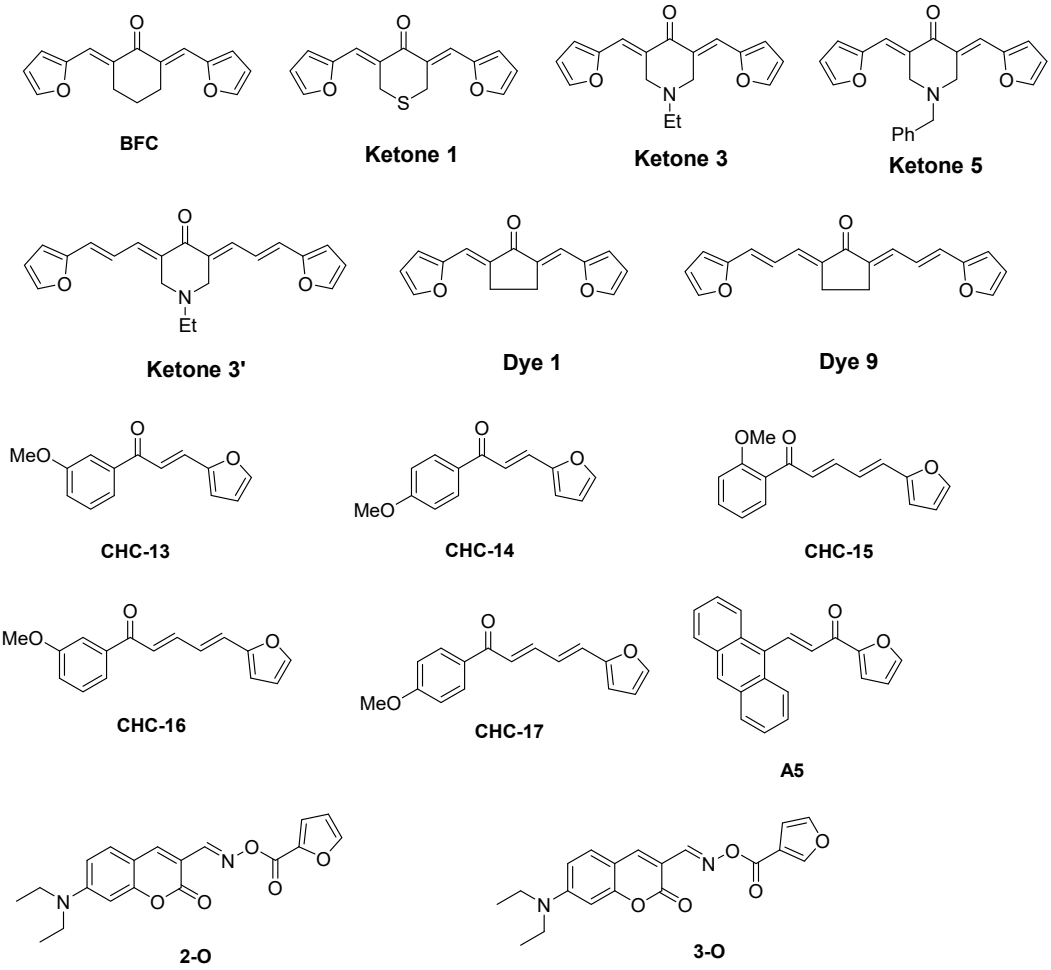

Figure 24. Chemical structures of the different furan-based compounds reported in this review.

At present, only three families of dyes have been designed with furane, namely, benzylidene ketones, chalcones, and coumarins. When incorporated in chalcones, the best position is undoubtedly on the acetophenone side, with the best monomer conversions being obtained in these conditions. In benzylidene ketones, photoinitiators that could be used in very low photoinitiator content could be prepared. Indeed, a concentration as low as 0.0625 wt% could be used. An efficient strategy has also been developed to elaborate water-soluble photoinitiators, consisting of preparing charge transfer complexes with triethanolamine. Future works will consist of multiplying the structures of water-soluble photoinitiators. Indeed, polymerization in more ecological conditions could be possible by using these photoinitiators. Photobleaching ability is also an important property for visible light photoinitiators as these molecules are strongly colored compounds [222]. Investigation of this property is the keypoint in order for visible light photoinitiators to be competitive with UV photopolymerization that only gives colorless coatings. However, future prospects will certainly consist of developing Type I photoinitiators based on furane. Indeed, if multicomponent photoinitiating systems have been popular in the past and extensively studied by numerous research groups, the extractability of photoinitiators and associated additives is more and more the focus of safety concerns, especially if applications, such as food packaging, are targeted. Additionally, performant photoinitiating systems have been reported in the past. However, performance was related to the use of three- and even four-component systems, complexifying the preparation of the resin. Conversely, Type I photoinitiators that are mono-component systems possess the unique ability to cleave upon photoexcitation. These structures could efficiently address the extractability issue through their ability to crosslink after photodecomposition and radical generation to

the polymer network. In this field, different structures can be envisioned such as oxime esters, phenyl glyoxylate derivatives, or diketones that can be obtained in a few synthetic steps and starting from cheap and easily available reagents [19].

Funding: Aix Marseille University and the Centre National de la Recherche Scientifique are greatly acknowledged for financial support under the frame of permanent fundings.

Data Availability Statement: No data are available for this work.

Acknowledgments: Aix Marseille University and the Centre National de la Recherche Scientifique are greatly acknowledged for financial support.

Conflicts of Interest: The authors declare no conflict of interest.

References

1. Jasinski, F.; Zetterlund, P.B.; Braun, A.M.; Chemtob, A. Photopolymerization in Dispersed Systems. *Prog. Polym. Sci.* **2018**, *84*, 47–88. [CrossRef]
2. Noè, C.; Hakkarainen, M.; Sangermano, M. Cationic UV-Curing of Epoxidized Biobased Resins. *Polymers* **2021**, *13*, 89. [CrossRef] [PubMed]
3. Yuan, Y.; Li, C.; Zhang, R.; Liu, R.; Liu, J. Low Volume Shrinkage Photopolymerization System Using Hydrogen-Bond-Based Monomers. *Prog. Org. Coat.* **2019**, *137*, 105308. [CrossRef]
4. Khudyakov, I.V.; Legg, J.C.; Purvis, M.B.; Overton, B.J. Kinetics of Photopolymerization of Acrylates with Functionality of 1−6. *Ind. Eng. Chem. Res.* **1999**, *38*, 3353–3359. [CrossRef]
5. Dickens, S.H.; Stansbury, J.W.; Choi, K.M.; Floyd, C.J.E. Photopolymerization Kinetics of Methacrylate Dental Resins. *Macromolecules* **2003**, *36*, 6043–6053. [CrossRef]
6. Maffezzoli, A.; Pietra, A.D.; Rengo, S.; Nicolais, L.; Valletta, G. Photopolymerization of Dental Composite Matrices. *Biomaterials* **1994**, *15*, 1221–1228. [CrossRef]
7. Dikova, T.; Maximov, J.; Todorov, V.; Georgiev, G.; Panov, V. Optimization of Photopolymerization Process of Dental Composites. *Processes* **2021**, *9*, 779. [CrossRef]
8. Andreu, A.; Su, P.-C.; Kim, J.-H.; Ng, C.S.; Kim, S.; Kim, I.; Lee, J.; Noh, J.; Subramanian, A.S.; Yoon, Y.-J. 4D Printing Materials for Vat Photopolymerization. *Addit. Manuf.* **2021**, *44*, 102024. [CrossRef]
9. Chen, H.; Noirbent, G.; Zhang, Y.; Sun, K.; Liu, S.; Brunel, D.; Gigmes, D.; Graff, B.; Morlet-Savary, F.; Xiao, P.; et al. Photopolymerization and 3D/4D Applications Using Newly Developed Dyes: Search around the Natural Chalcone Scaffold in Photoinitiating Systems. *Dyes Pigments* **2021**, *188*, 109213. [CrossRef]
10. Bagheri, A.; Jin, J. Photopolymerization in 3D Printing. *ACS Appl. Polym. Mater.* **2019**, *1*, 593–611. [CrossRef]
11. Lalevée, J.; Fouassier, J.-P. *Dyes and Chromophores in Polymer Science*; ISTE Ltd. and John Wiley & Sons Inc.: Hoboken, NJ, USA, 2015; ISBN 978-1-84821-742-3.
12. Belon, C.; Allonas, X.; Croutxé-barghorn, C.; Lalevée, J. Overcoming the Oxygen Inhibition in the Photopolymerization of Acrylates: A Study of the Beneficial Effect of Triphenylphosphine. *J. Polym. Sci. Part Polym. Chem.* **2010**, *48*, 2462–2469. [CrossRef]
13. Lalevée, J.; Mokbel, H.; Fouassier, J.-P. Recent Developments of Versatile Photoinitiating Systems for Cationic Ring Opening Polymerization Operating at Any Wavelengths and under Low Light Intensity Sources. *Molecules* **2015**, *20*, 7201–7221. [CrossRef] [PubMed]
14. Xiao, P.; Dumur, F.; Thirion, D.; Fagour, S.; Vacher, A.; Sallenave, X.; Morlet-Savary, F.; Graff, B.; Fouassier, J.P.; Gigmes, D.; et al. Multicolor Photoinitiators for Radical and Cationic Polymerization: Monofunctional vs Polyfunctional Thiophene Derivatives. *Macromolecules* **2013**, *46*, 6786–6793. [CrossRef]
15. Lalevée, J.; Telitel, S.; Xiao, P.; Lepeltier, M.; Dumur, F.; Morlet-Savary, F.; Gigmes, D.; Fouassier, J.-P. Metal and Metal-Free Photocatalysts: Mechanistic Approach and Application as Photoinitiators of Photopolymerization. *Beilstein J. Org. Chem.* **2014**, *10*, 863–876. [CrossRef] [PubMed]
16. Noirbent, G.; Dumur, F. Photoinitiators of Polymerization with Reduced Environmental Impact: Nature as an Unlimited and Renewable Source of Dyes. *Eur. Polym. J.* **2021**, *142*, 110109. [CrossRef]
17. Kim, K.; Sinha, J.; Gao, G.; Childress, K.K.; Sartor, S.M.; Salazar, A.M.; Huang, S.; Musgrave, C.B.; Stansbury, J.W. High-Efficiency Radical Photopolymerization Enhanced by Autonomous Dark Cure. *Macromolecules* **2020**, *53*, 5034–5046. [CrossRef]
18. Shaukat, U.; Sölle, B.; Rossegger, E.; Rana, S.; Schlögl, S. Vat Photopolymerization 3D-Printing of Dynamic Thiol-Acrylate Photopolymers Using Bio-Derived Building Blocks. *Polymers* **2022**, *14*, 5377. [CrossRef]
19. Müller, S.M.; Schlögl, S.; Wiesner, T.; Haas, M.; Griesser, T. Recent Advances in Type I Photoinitiators for Visible Light Induced Photopolymerization. *ChemPhotoChem* **2022**, *6*, e202200091. [CrossRef]
20. Petko, F.; Świeży, A.; Ortyl, J. Photoinitiating Systems and Kinetics of Frontal Photopolymerization Processes—The Prospects for Efficient Preparation of Composites and Thick 3D Structures. *Polym. Chem.* **2021**, *12*, 4593–4612. [CrossRef]
21. Tehfe, M.A.; Louradour, F.; Lalevée, J.; Fouassier, J.-P. Photopolymerization Reactions: On the Way to a Green and Sustainable Chemistry. *Appl. Sci.* **2013**, *3*, 490–514. [CrossRef]

22. Awwad, N.; Bui, A.T.; Danilov, E.O.; Castellano, F.N. Visible-Light-Initiated Free-Radical Polymerization by Homomolecular Triplet-Triplet Annihilation. *Chem* **2020**, *6*, 3071–3085. [CrossRef]
23. Tomal, W.; Ortyl, J. Water-Soluble Photoinitiators in Biomedical Applications. *Polymers* **2020**, *12*, 1073. [CrossRef] [PubMed]
24. Fiedor, P.; Pilch, M.; Szymaszek, P.; Chachaj-Brekiesz, A.; Galek, M.; Ortyl, J. Photochemical Study of a New Bimolecular Photoinitiating System for Vat Photopolymerization 3D Printing Techniques under Visible Light. *Catalysts* **2020**, *10*, 284. [CrossRef]
25. Hola, E.; Fiedor, P.; Dzienia, A.; Ortyl, J. Visible-Light Amine Thioxanthone Derivatives as Photoredox Catalysts for Photopolymerization Processes. *ACS Appl. Polym. Mater.* **2021**, *3*, 5547–5558. [CrossRef]
26. Hola, E.; Topa, M.; Chachaj-Brekiesz, A.; Pilch, M.; Fiedor, P.; Galek, M.; Ortyl, J. New, Highly Versatile Bimolecular Photoinitiating Systems for Free-Radical, Cationic and Thiol–Ene Photopolymerization Processes under Low Light Intensity UV and Visible LEDs for 3D Printing Application. *RSC Adv.* **2020**, *10*, 7509–7522. [CrossRef]
27. Xiao, P.; Dumur, F.; Graff, B.; Morlet-Savary, F.; Vidal, L.; Gigmes, D.; Fouassier, J.P.; Lalevée, J. Structural Effects in the Indanedione Skeleton for the Design of Low Intensity 300–500 Nm Light Sensitive Initiators. *Macromolecules* **2014**, *47*, 26–34. [CrossRef]
28. Fouassier, J.P.; Lalevée, J. Three-Component Photoinitiating Systems: Towards Innovative Tailor Made High Performance Combinations. *RSC Adv.* **2012**, *2*, 2621–2629. [CrossRef]
29. Lalevée, J.; Blanchard, N.; Tehfe, M.A.; Fries, C.; Morlet-Savary, F.; Gigmes, D.; Fouassier, J.P. New Thioxanthone and Xanthone Photoinitiators Based on Silyl Radical Chemistry. *Polym. Chem.* **2011**, *2*, 1077–1084. [CrossRef]
30. Lalevée, J.; Telitel, S.; Tehfe, M.A.; Fouassier, J.P.; Curran, D.P.; Lacôte, E. N-Heterocyclic Carbene Boranes Accelerate Type I Radical Photopolymerizations and Overcome Oxygen Inhibition. *Angew. Chem. Int. Ed.* **2012**, *51*, 5958–5961. [CrossRef]
31. Dietlin, C.; Schweizer, S.; Xiao, P.; Zhang, J.; Morlet-Savary, F.; Graff, B.; Fouassier, J.-P.; Lalevée, J. Photopolymerization upon LEDs: New Photoinitiating Systems and Strategies. *Polym. Chem.* **2015**, *6*, 3895–3912. [CrossRef]
32. Liu, S.; Borjigin, T.; Schmitt, M.; Morlet-Savary, F.; Xiao, P.; Lalevée, J. High-Performance Photoinitiating Systems for LED-Induced Photopolymerization. *Polymers* **2023**, *15*, 342. [CrossRef] [PubMed]
33. Jandt, K.D.; Mills, R.W. A Brief History of LED Photopolymerization. *Dent. Mater.* **2013**, *29*, 605–617. [CrossRef] [PubMed]
34. Gallastegui, A.; Dominguez-Alfaro, A.; Lezama, L.; Alegret, N.; Prato, M.; Gómez, M.L.; Mecerreyes, D. Fast Visible-Light Photopolymerization in the Presence of Multiwalled Carbon Nanotubes: Toward 3D Printing Conducting Nanocomposites. *ACS Macro Lett.* **2022**, *11*, 303–309. [CrossRef] [PubMed]
35. Peng, X.; Zhang, J.; Banaszak Holl, M.M.; Xiao, P. Thiol-Ene Photopolymerization under Blue, Green and Red LED Irradiation. *ChemPhotoChem* **2021**, *5*, 571–581. [CrossRef]
36. Armstrong, B.K.; Kricker, A. The Epidemiology of UV Induced Skin Cancer. *Consequences Expo. Sunlightelements Assess Prot.* **2001**, *63*, 8–18. [CrossRef] [PubMed]
37. de Gruijl, F.R. Skin Cancer and Solar UV Radiation. *Eur. J. Cancer* **1999**, *35*, 2003–2009. [CrossRef]
38. Narayanan, D.L.; Saladi, R.N.; Fox, J.L. Review: Ultraviolet Radiation and Skin Cancer. *Int. J. Dermatol.* **2010**, *49*, 978–986. [CrossRef]
39. Shao, J.; Huang, Y.; Fan, Q. Visible Light Initiating Systems for Photopolymerization: Status, Development and Challenges. *Polym. Chem.* **2014**, *5*, 4195–4210. [CrossRef]
40. Bonardi, A.H.; Dumur, F.; Grant, T.M.; Noirbent, G.; Gigmes, D.; Lessard, B.H.; Fouassier, J.-P.; Lalevée, J. High Performance Near-Infrared (NIR) Photoinitiating Systems Operating under Low Light Intensity and in the Presence of Oxygen. *Macromolecules* **2018**, *51*, 1314–1324. [CrossRef]
41. Zivic, N.; Bouzrati-Zerrelli, M.; Villotte, S.; Morlet-Savary, F.; Dietlin, C.; Dumur, F.; Gigmes, D.; Fouassier, J.P.; Lalevée, J. A Novel Naphthalimide Scaffold Based Iodonium Salt as a One-Component Photoacid/Photoinitiator for Cationic and Radical Polymerization under LED Exposure. *Polym. Chem.* **2016**, *7*, 5873–5879. [CrossRef]
42. Bonardi, A.-H.; Zahouily, S.; Dietlin, C.; Graff, B.; Morlet-Savary, F.; Ibrahim-Ouali, M.; Gigmes, D.; Hoffmann, N.; Dumur, F.; Lalevée, J. New 1,8-Naphthalimide Derivatives as Photoinitiators for Free-Radical Polymerization Upon Visible Light. *Catalysts* **2019**, *9*, 637. [CrossRef]
43. Zhang, J.; Zivic, N.; Dumur, F.; Xiao, P.; Graff, B.; Fouassier, J.P.; Gigmes, D.; Lalevée, J. Naphthalimide-Tertiary Amine Derivatives as Blue-Light-Sensitive Photoinitiators. *ChemPhotoChem* **2018**, *2*, 481–489. [CrossRef]
44. Xiao, P.; Dumur, F.; Zhang, J.; Graff, B.; Gigmes, D.; Fouassier, J.P.; Lalevée, J. Naphthalimide Derivatives: Substituent Effects on the Photoinitiating Ability in Polymerizations under Near UV, Purple, White and Blue LEDs (385, 395, 405, 455, or 470 Nm). *Macromol. Chem. Phys.* **2015**, *216*, 1782–1790. [CrossRef]
45. Xiao, P.; Dumur, F.; Zhang, J.; Graff, B.; Gigmes, D.; Fouassier, J.P.; Lalevée, J. Naphthalimide-Phthalimide Derivative Based Photoinitiating Systems for Polymerization Reactions under Blue Lights. *J. Polym. Sci. Part Polym. Chem.* **2015**, *53*, 665–674. [CrossRef]
46. Zhang, J.; Zivic, N.; Dumur, F.; Xiao, P.; Graff, B.; Gigmes, D.; Fouassier, J.P.; Lalevée, J. A Benzophenone-Naphthalimide Derivative as Versatile Photoinitiator of Polymerization under near UV and Visible Lights. *J. Polym. Sci. Part Polym. Chem.* **2015**, *53*, 445–451. [CrossRef]
47. Zhang, J.; Zivic, N.; Dumur, F.; Xiao, P.; Graff, B.; Fouassier, J.P.; Gigmes, D.; Lalevée, J. N-[2-(Dimethylamino)Ethyl]-1,8-Naphthalimide Derivatives as Photoinitiators under LEDs. *Polym. Chem.* **2018**, *9*, 994–1003. [CrossRef]

48. Zhang, J.; Dumur, F.; Xiao, P.; Graff, B.; Bardelang, D.; Gigmes, D.; Fouassier, J.P.; Lalevée, J. Structure Design of Naphthalimide Derivatives: Toward Versatile Photoinitiators for Near-UV/Visible LEDs, 3D Printing, and Water-Soluble Photoinitiating Systems. *Macromolecules* **2015**, *48*, 2054–2063. [CrossRef]
49. Zhang, J.; Zivic, N.; Dumur, F.; Xiao, P.; Graff, B.; Fouassier, J.P.; Gigmes, D.; Lalevée, J. UV-Violet-Blue LED Induced Polymerizations: Specific Photoinitiating Systems at 365, 385, 395 and 405 Nm. *Polymer* **2014**, *55*, 6641–6648. [CrossRef]
50. Xiao, P.; Dumur, F.; Graff, B.; Gigmes, D.; Fouassier, J.P.; Lalevée, J. Blue Light Sensitive Dyes for Various Photopolymerization Reactions: Naphthalimide and Naphthalic Anhydride Derivatives. *Macromolecules* **2014**, *47*, 601–608. [CrossRef]
51. Xiao, P.; Dumur, F.; Frigoli, M.; Tehfe, M.-A.; Graff, B.; Fouassier, J.P.; Gigmes, D.; Lalevée, J. Naphthalimide Based Methacrylated Photoinitiators in Radical and Cationic Photopolymerization under Visible Light. *Polym. Chem.* **2013**, *4*, 5440–5448. [CrossRef]
52. Noirbent, G.; Dumur, F. Recent Advances on Naphthalic Anhydrides and 1,8-Naphthalimide-Based Photoinitiators of Polymerization. *Eur. Polym. J.* **2020**, *132*, 109702. [CrossRef]
53. Rahal, M.; Mokbel, H.; Graff, B.; Pertici, V.; Gigmes, D.; Toufaily, J.; Hamieh, T.; Dumur, F.; Lalevée, J. Naphthalimide-Based Dyes as Photoinitiators under Visible Light Irradiation and Their Applications: Photocomposite Synthesis, 3D Printing and Polymerization in Water. *ChemPhotoChem* **2021**, *5*, 476–490. [CrossRef]
54. Rahal, M.; Graff, B.; Toufaily, J.; Hamieh, T.; Ibrahim-Ouali, M.; Dumur, F.; Lalevée, J. Naphthyl-Naphthalimides as High-Performance Visible Light Photoinitiators for 3D Printing and Photocomposites Synthesis. *Catalysts* **2021**, *11*, 1269. [CrossRef]
55. Zivic, N.; Zhang, J.; Bardelang, D.; Dumur, F.; Xiao, P.; Jet, T.; Versace, D.-L.; Dietlin, C.; Morlet-Savary, F.; Graff, B.; et al. Novel Naphthalimide–Amine Based Photoinitiators Operating under Violet and Blue LEDs and Usable for Various Polymerization Reactions and Synthesis of Hydrogels. *Polym. Chem.* **2015**, *7*, 418–429. [CrossRef]
56. Xiao, P.; Dumur, F.; Graff, B.; Morlet-Savary, F.; Gigmes, D.; Fouassier, J.P.; Lalevée, J. Design of High Performance Photoinitiators at 385–405 Nm: Search around the Naphthalene Scaffold. *Macromolecules* **2014**, *47*, 973–978. [CrossRef]
57. Xiao, P.; Dumur, F.; Zhang, J.; Graff, B.; Gigmes, D.; Fouassier, J.P.; Lalevée, J. Amino and Nitro Substituted 2-Amino-1H-Benzo[de]Isoquinoline-1,3(2H)-Diones: As Versatile Photoinitiators of Polymerization from Violet-Blue LED Absorption to a Panchromatic Behavior. *Polym. Chem.* **2015**, *6*, 1171–1179. [CrossRef]
58. Chen, H.; Pieuchot, L.; Xiao, P.; Dumur, F.; Lalevée, J. Water-Soluble/Visible-Light-Sensitive Naphthalimide Derivative-Based Photoinitiating Systems: 3D Printing of Antibacterial Hydrogels. *Polym. Chem.* **2022**, *13*, 2918–2932. [CrossRef]
59. Liu, S.; Giacoletto, N.; Graff, B.; Morlet-Savary, F.; Nechab, M.; Xiao, P.; Dumur, F.; Lalevée, J. N-Naphthalimide Ester Derivatives as Type I Photoinitiators for LED Photopolymerization. *Mater. Today Chem.* **2022**, *26*, 101137. [CrossRef]
60. Tehfe, M.-A.; Dumur, F.; Contal, E.; Graff, B.; Morlet-Savary, F.; Gigmes, D.; Fouassier, J.-P.; Lalevée, J. New Insights into Radical and Cationic Polymerizations upon Visible Light Exposure: Role of Novel Photoinitiator Systems Based on the Pyrene Chromophore. *Polym. Chem.* **2013**, *4*, 1625–1634. [CrossRef]
61. Telitel, S.; Dumur, F.; Faury, T.; Graff, B.; Tehfe, M.-A.; Gigmes, D.; Fouassier, J.-P.; Lalevée, J. New Core-Pyrene π Structure Organophotocatalysts Usable as Highly Efficient Photoinitiators. *Beilstein J. Org. Chem.* **2013**, *9*, 877–890. [CrossRef]
62. Uchida, N.; Nakano, H.; Igarashi, T.; Sakurai, T. Nonsalt 1-(Arylmethyloxy)Pyrene Photoinitiators Capable of Initiating Cationic Polymerization. *J. Appl. Polym. Sci.* **2014**, *131*. [CrossRef]
63. Mishra, A.; Daswal, S. 1-(Bromoacetyl)Pyrene, a Novel Photoinitiator for the Copolymerization of Styrene and Methylmethacrylate. *Radiat. Phys. Chem.* **2006**, *75*, 1093–1100. [CrossRef]
64. Tehfe, M.-A.; Dumur, F.; Graff, B.; Morlet-Savary, F.; Gigmes, D.; Fouassier, J.-P.; Lalevée, J. Design of New Type I and Type II Photoinitiators Possessing Highly Coupled Pyrene–Ketone Moieties. *Polym. Chem.* **2013**, *4*, 2313–2324. [CrossRef]
65. Dumur, F. Recent Advances on Pyrene-Based Photoinitiators of Polymerization. *Eur. Polym. J.* **2020**, *126*, 109564. [CrossRef]
66. Tehfe, M.-A.; Dumur, F.; Vilà, N.; Graff, B.; Mayer, C.R.; Fouassier, J.P.; Gigmes, D.; Lalevée, J. A Multicolor Photoinitiator for Cationic Polymerization and Interpenetrated Polymer Network Synthesis: 2,7-Di-Tert-Butyldimethyldihydropyrene. *Macromol. Rapid Commun.* **2013**, *34*, 1104–1109. [CrossRef] [PubMed]
67. Telitel, S.; Dumur, F.; Gigmes, D.; Graff, B.; Fouassier, J.P.; Lalevée, J. New Functionalized Aromatic Ketones as Photoinitiating Systems for near Visible and Visible Light Induced Polymerizations. *Polymer* **2013**, *54*, 2857–2864. [CrossRef]
68. Tehfe, M.-A.; Lalevée, J.; Telitel, S.; Contal, E.; Dumur, F.; Gigmes, D.; Bertin, D.; Nechab, M.; Graff, B.; Morlet-Savary, F.; et al. Polyaromatic Structures as Organo-Photoinitiator Catalysts for Efficient Visible Light Induced Dual Radical/Cationic Photopolymerization and Interpenetrated Polymer Networks Synthesis. *Macromolecules* **2012**, *45*, 4454–4460. [CrossRef]
69. Liu, S.; Chen, H.; Zhang, Y.; Sun, K.; Xu, Y.; Morlet-Savary, F.; Graff, B.; Noirbent, G.; Pigot, C.; Brunel, D.; et al. Monocomponent Photoinitiators Based on Benzophenone-Carbazole Structure for LED Photoinitiating Systems and Application on 3D Printing. *Polymers* **2020**, *12*, 1394. [CrossRef]
70. Xiao, P.; Dumur, F.; Graff, B.; Gigmes, D.; Fouassier, J.P.; Lalevée, J. Variations on the Benzophenone Skeleton: Novel High Performance Blue Light Sensitive Photoinitiating Systems. *Macromolecules* **2013**, *46*, 7661–7667. [CrossRef]
71. Zhang, J.; Frigoli, M.; Dumur, F.; Xiao, P.; Ronchi, L.; Graff, B.; Morlet-Savary, F.; Fouassier, J.P.; Gigmes, D.; Lalevée, J. Design of Novel Photoinitiators for Radical and Cationic Photopolymerizations under Near UV and Visible LEDs (385, 395, and 405 Nm). *Macromolecules* **2014**, *47*, 2811–2819. [CrossRef]
72. Liu, S.; Brunel, D.; Noirbent, G.; Mau, A.; Chen, H.; Morlet-Savary, F.; Graff, B.; Gigmes, D.; Xiao, P.; Dumur, F.; et al. New Multifunctional Benzophenone-Based Photoinitiators with High Migration Stability and Their Applications in 3D Printing. *Mater. Chem. Front.* **2021**, *5*, 1982–1994. [CrossRef]

73. Liu, S.; Brunel, D.; Sun, K.; Zhang, Y.; Chen, H.; Xiao, P.; Dumur, F.; Lalevée, J. Novel Photoinitiators Based on Benzophenone-Triphenylamine Hybrid Structure for LED Photopolymerization. *Macromol. Rapid Commun.* **2020**, *41*, 2000460. [CrossRef] [PubMed]
74. Liu, S.; Brunel, D.; Sun, K.; Xu, Y.; Morlet-Savary, F.; Graff, B.; Xiao, P.; Dumur, F.; Lalevée, J. A Monocomponent Bifunctional Benzophenone–Carbazole Type II Photoinitiator for LED Photoinitiating Systems. *Polym. Chem.* **2020**, *11*, 3551–3556. [CrossRef]
75. Tehfe, M.-A.; Dumur, F.; Graff, B.; Morlet-Savary, F.; Fouassier, J.-P.; Gigmes, D.; Lalevée, J. Trifunctional Photoinitiators Based on a Triazine Skeleton for Visible Light Source and UV LED Induced Polymerizations. *Macromolecules* **2012**, *45*, 8639–8647. [CrossRef]
76. Lin, J.-T.; Lalevee, J. Efficacy Modeling of New Multi-Functional Benzophenone-Based System for Free-Radical/Cationic Hybrid Photopolymerization Using 405 Nm LED. 2021, 29, 100. *J. Polym. Res.* **2021**, *29*, 100. [CrossRef]
77. Zhang, J.; Campolo, D.; Dumur, F.; Xiao, P.; Gigmes, D.; Fouassier, J.P.; Lalevée, J. The Carbazole-Bound Ferrocenium Salt as a Specific Cationic Photoinitiator upon near-UV and Visible LEDs (365–405 Nm). *Polym. Bull.* **2016**, *73*, 493–507. [CrossRef]
78. Al Mousawi, A.; Dumur, F.; Garra, P.; Toufaily, J.; Hamieh, T.; Graff, B.; Gigmes, D.; Fouassier, J.P.; Lalevée, J. Carbazole Scaffold Based Photoinitiator/Photoredox Catalysts: Toward New High Performance Photoinitiating Systems and Application in LED Projector 3D Printing Resins. *Macromolecules* **2017**, *50*, 2747–2758. [CrossRef]
79. Al Mousawi, A.; Lara, D.M.; Noirbent, G.; Dumur, F.; Toufaily, J.; Hamieh, T.; Bui, T.-T.; Goubard, F.; Graff, B.; Gigmes, D.; et al. Carbazole Derivatives with Thermally Activated Delayed Fluorescence Property as Photoinitiators/Photoredox Catalysts for LED 3D Printing Technology. *Macromolecules* **2017**, *50*, 4913–4926. [CrossRef]
80. Al Mousawi, A.; Garra, P.; Dumur, F.; Bui, T.-T.; Goubard, F.; Toufaily, J.; Hamieh, T.; Graff, B.; Gigmes, D.; Fouassier, J.P.; et al. Novel Carbazole Skeleton-Based Photoinitiators for LED Polymerization and LED Projector 3D Printing. *Molecules* **2017**, *22*, 2143. [CrossRef]
81. Mousawi, A.A.; Arar, A.; Ibrahim-Ouali, M.; Duval, S.; Dumur, F.; Garra, P.; Toufaily, J.; Hamieh, T.; Graff, B.; Gigmes, D.; et al. Carbazole-Based Compounds as Photoinitiators for Free Radical and Cationic Polymerization upon near Visible Light Illumination. *Photochem. Photobiol. Sci.* **2018**, *17*, 578–585. [CrossRef]
82. Abdallah, M.; Magaldi, D.; Hijazi, A.; Graff, B.; Dumur, F.; Fouassier, J.-P.; Bui, T.-T.; Goubard, F.; Lalevée, J. Development of New High-Performance Visible Light Photoinitiators Based on Carbazole Scaffold and Their Applications in 3d Printing and Photocomposite Synthesis. *J. Polym. Sci. Part Polym. Chem.* **2019**, *57*, 2081–2092. [CrossRef]
83. Dumur, F. Recent Advances on Carbazole-Based Photoinitiators of Polymerization. *Eur. Polym. J.* **2020**, *125*, 109503. [CrossRef]
84. Liu, S.; Graff, B.; Xiao, P.; Dumur, F.; Lalevée, J. Nitro-Carbazole Based Oxime Esters as Dual Photo/Thermal Initiators for 3D Printing and Composite Preparation. *Macromol. Rapid Commun.* **2021**, *42*, 2100207. [CrossRef] [PubMed]
85. Hammoud, F.; Hijazi, A.; Duval, S.; Lalevée, J.; Dumur, F. 5,12-Dihydroindolo[3,2-a]Carbazole: A Promising Scaffold for the Design of Visible Light Photoinitiators of Polymerization. *Eur. Polym. J.* **2022**, *162*, 110880. [CrossRef]
86. Liu, S.; Giacoletto, N.; Schmitt, M.; Nechab, M.; Graff, B.; Morlet-Savary, F.; Xiao, P.; Dumur, F.; Lalevée, J. Effect of Decarboxylation on the Photoinitiation Behavior of Nitrocarbazole-Based Oxime Esters. *Macromolecules* **2022**, *55*, 2475–2485. [CrossRef]
87. Hammoud, F.; Hijazi, A.; Ibrahim-Ouali, M.; Lalevée, J.; Dumur, F. Chemical Engineering around the 5,12-Dihydroindolo[3,2-a]Carbazole Scaffold: Fine Tuning of the Optical Properties of Visible Light Photoinitiators of Polymerization. *Eur. Polym. J.* **2022**, *172*, 111218. [CrossRef]
88. Xu, C.; Gong, S.; Wu, X.; Wu, Y.; Liao, Q.; Xiong, Y.; Li, Z.; Tang, H. High-Efficient Carbazole-Based Photo-Bleachable Dyes as Free Radical Initiators for Visible Light Polymerization. *Dyes Pigments* **2022**, *198*, 110039. [CrossRef]
89. Dumur, F. Recent Advances on Carbazole-Based Oxime Esters as Photoinitiators of Polymerization. *Eur. Polym. J.* **2022**, *175*, 111330. [CrossRef]
90. Hammoud, F.; Giacoletto, N.; Nechab, M.; Graff, B.; Hijazi, A.; Dumur, F.; Lalevée, J. 5,12-Dialkyl-5,12-Dihydroindolo[3,2-a]Carbazole-Based Oxime-Esters for LED Photoinitiating Systems and Application on 3D Printing. *Macromol. Mater. Eng.* **2022**, *307*, 2200082. [CrossRef]
91. Karaca, N.; Ocal, N.; Arsu, N.; Jockusch, S. Thioxanthone-Benzothiophenes as Photoinitiator for Free Radical Polymerization. *J. Photochem. Photobiol. Chem.* **2016**, *331*, 22–28. [CrossRef]
92. Balta, D.K.; Cetiner, N.; Temel, G.; Turgut, Z.; Arsu, N. An Annelated Thioxanthone as a New Type II Initiator. *J. Photochem. Photobiol. Chem.* **2008**, *199*, 316–321. [CrossRef]
93. Balta, D.K.; Temel, G.; Goksu, G.; Ocal, N.; Arsu, N. Thioxanthone–Diphenyl Anthracene: Visible Light Photoinitiator. *Macromolecules* **2012**, *45*, 119–125. [CrossRef]
94. Dadashi-Silab, S.; Aydogan, C.; Yagci, Y. Shining a Light on an Adaptable Photoinitiator: Advances in Photopolymerizations Initiated by Thioxanthones. *Polym. Chem.* **2015**, *6*, 6595–6615. [CrossRef]
95. Eren, T.N.; Yasar, N.; Aviyente, V.; Morlet-Savary, F.; Graff, B.; Fouassier, J.P.; Lalevee, J.; Avci, D. Photophysical and Photochemical Studies of Novel Thioxanthone-Functionalized Methacrylates through LED Excitation. *Macromol. Chem. Phys.* **2016**, *217*, 1501–1512. [CrossRef]
96. Qiu, J.; Wei, J. Thioxanthone Photoinitiator Containing Polymerizable N-Aromatic Maleimide for Photopolymerization. *J. Polym. Res.* **2014**, *21*, 559. [CrossRef]
97. Tar, H.; Sevinc Esen, D.; Aydin, M.; Ley, C.; Arsu, N.; Allonas, X. Panchromatic Type II Photoinitiator for Free Radical Polymerization Based on Thioxanthone Derivative. *Macromolecules* **2013**, *46*, 3266–3272. [CrossRef]

98. Wu, Q.; Wang, X.; Xiong, Y.; Yang, J.; Tang, H. Thioxanthone Based One-Component Polymerizable Visible Light Photoinitiator for Free Radical Polymerization. *RSC Adv.* **2016**, *6*, 66098–66107. [CrossRef]
99. Wu, Q.; Tang, K.; Xiong, Y.; Wang, X.; Yang, J.; Tang, H. High-Performance and Low Migration One-Component Thioxanthone Visible Light Photoinitiators. *Macromol. Chem. Phys.* **2017**, *218*, 1600484. [CrossRef]
100. Wu, X.; Jin, M.; Malval, J.-P.; Wan, D.; Pu, H. Visible Light-Emitting Diode-Sensitive Thioxanthone Derivatives Used in Versatile Photoinitiating Systems for Photopolymerizations. *J. Polym. Sci. Part Polym. Chem.* **2017**, *55*, 4037–4045. [CrossRef]
101. Lalevée, J.; Tehfe, M.-A.; Dumur, F.; Gigmes, D.; Graff, B.; Morlet-Savary, F.; Fouassier, J.-P. Light-Harvesting Organic Photoinitiators of Polymerization. *Macromol. Rapid Commun.* **2013**, *34*, 239–245. [CrossRef]
102. Esen, D.S.; Karasu, F.; Arsu, N. The Investigation of Photoinitiated Polymerization of Multifunctional Acrylates with TX-BT by Photo-DSC and RT-FTIR. *Prog. Org. Coat.* **2011**, *70*, 102–107. [CrossRef]
103. Gencoglu, T.; Eren, T.N.; Lalevée, J.; Avci, D. A Water Soluble, Low Migration, and Visible Light Photoinitiator by Thioxanthone-Functionalization of Poly(Ethylene Glycol)-Containing Poly(β-Amino Ester). *Macromol. Chem. Phys.* **2022**, *223*, 2100450. [CrossRef]
104. Kamoun, E.A.; Winkel, A.; Eisenburger, M.; Menzel, H. Carboxylated Camphorquinone as Visible-Light Photoinitiator for Biomedical Application: Synthesis, Characterization, and Application. *Arab. J. Chem.* **2016**, *9*, 745–754. [CrossRef]
105. Santini, A.; Gallegos, I.T.; Felix, C.M. Photoinitiators in Dentistry: A Review. *Prim. Dent. J.* **2013**, *2*, 30–33. [CrossRef] [PubMed]
106. Zhao, J.; Lalevée, J.; Lu, H.; MacQueen, R.; Kable, S.H.; Schmidt, T.W.; Stenzel, M.H.; Xiao, P. A New Role of Curcumin: As a Multicolor Photoinitiator for Polymer Fabrication under Household UV to Red LED Bulbs. *Polym. Chem.* **2015**, *6*, 5053–5061. [CrossRef]
107. Crivello, J.V.; Bulut, U. Curcumin: A Naturally Occurring Long-Wavelength Photosensitizer for Diaryliodonium Salts. *J. Polym. Sci. Part Polym. Chem.* **2005**, *43*, 5217–5231. [CrossRef]
108. Han, W.; Fu, H.; Xue, T.; Liu, T.; Wang, Y.; Wang, T. Facilely Prepared Blue-Green Light Sensitive Curcuminoids with Excellent Bleaching Properties as High Performance Photosensitizers in Cationic and Free Radical Photopolymerization. *Polym. Chem.* **2018**, *9*, 1787–1798. [CrossRef]
109. Mishra, A.; Daswal, S. Curcumin, A Novel Natural Photoinitiator for the Copolymerization of Styrene and Methylmethacrylate. *J. Macromol. Sci. Part A* **2005**, *42*, 1667–1678. [CrossRef]
110. Zhang, J.; Lalevée, J.; Zhao, J.; Graff, B.; Stenzel, M.H.; Xiao, P. Dihydroxyanthraquinone Derivatives: Natural Dyes as Blue-Light-Sensitive Versatile Photoinitiators of Photopolymerization. *Polym. Chem.* **2016**, *7*, 7316–7324. [CrossRef]
111. Kirschner, J.; Baralle, A.; Paillard, J.; Graff, B.; Becht, J.-M.; Klee, J.E.; Lalevée, J. Silyl Glyoximides: Toward a New Class of Visible Light Photoinitiators. *Macromol. Chem. Phys.* **2022**, *223*, 2100500. [CrossRef]
112. Mokbel, H.; Toufaily, J.; Hamieh, T.; Dumur, F.; Campolo, D.; Gigmes, D.; Fouassier, J.P.; Ortyl, J.; Lalevée, J. Specific Cationic Photoinitiators for near UV and Visible LEDs: Iodonium versus Ferrocenium Structures. *J. Appl. Polym. Sci.* **2015**, *132*, 42759. [CrossRef]
113. Villotte, S.; Gigmes, D.; Dumur, F.; Lalevée, J. Design of Iodonium Salts for UV or Near-UV LEDs for Photoacid Generator and Polymerization Purposes. *Molecules* **2020**, *25*, 149. [CrossRef] [PubMed]
114. Tasdelen, M.A.; Kumbaraci, V.; Jockusch, S.; Turro, N.J.; Talinli, N.; Yagci, Y. Photoacid Generation by Stepwise Two-Photon Absorption: Photoinitiated Cationic Polymerization of Cyclohexene Oxide by Using Benzodioxinone in the Presence of Iodonium Salt. *Macromolecules* **2008**, *41*, 295–297. [CrossRef]
115. Crivello, J.V.; Lam, J.H.W. Diaryliodonium Salts. A New Class of Photoinitiators for Cationic Polymerization. *Macromolecules* **1977**, *10*, 1307–1315. [CrossRef]
116. He, Y.; Zhou, W.; Wu, F.; Li, M.; Wang, E. Photoreaction and Photopolymerization Studies on Squaraine Dyes/Iodonium Salts Combination. *J. Photochem. Photobiol. Chem.* **2004**, *162*, 463–471. [CrossRef]
117. Jun, L.I.; Miaozhen, L.I.; Huaihai, S.; Yongyuan, Y.; Erjian, W. Photopolymerization Initiated by Dimethylaminochalcone/Diphenyliodonium Salt Combination System Sensitive to Visible Light. *Chin. J Polym Sci* **1993**, *11*, 163–170.
118. Zivic, N.; Kuroishi, P.K.; Dumur, F.; Gigmes, D.; Dove, A.P.; Sardon, H. Recent Advances and Challenges in the Design of Organic Photoacid and Photobase Generators for Polymerizations. *Angew. Chem. Int. Ed.* **2019**, *58*, 10410–10422. [CrossRef]
119. Dumur, F. Recent Advances on Visible Light Phenothiazine-Based Photoinitiators of Polymerization. *Eur. Polym. J.* **2022**, *165*, 110999. [CrossRef]
120. Deng, L.; Tang, L.; Qu, J. Novel Chalcone-Based Phenothiazine Derivative Photoinitiators for Visible Light Induced Photopolymerization with Photobleaching and Good Biocompatibility. *Prog. Org. Coat.* **2022**, *167*, 106859. [CrossRef]
121. Rahal, M.; Abdallah, M.; Bui, T.-T.; Goubard, F.; Graff, B.; Dumur, F.; Toufaily, J.; Hamieh, T.; Lalevée, J. Design of New Phenothiazine Derivatives as Visible Light Photoinitiators. *Polym. Chem.* **2020**, *11*, 3349–3359. [CrossRef]
122. Li, S.; Hu, J.; Zhang, S.; Feng, C.; Zhang, L.; Wang, C.; He, Z.; Zhang, L. Novel A-π-D-π-A Structure Two-Photon Polymerization Initiators Based on Phenothiazine and Carbazole Derivatives. *Chem. Pap.* **2021**, *75*, 5249–5256. [CrossRef]
123. Grishin, D.F.; Lizyakina, O.S.; Vaganova, L.B.; Kaltenberg, A.A.; Grishin, I.D. Radical Polymerization of Methyl Methacrylate in the Presence of Methylene Blue and Organobromides under Visible Light Irradiation. *Iran. Polym. J.* **2021**, *30*, 1117–1126. [CrossRef]
124. Xu, D.; Zou, X.; Zhu, Y.; Yu, Z.; Jin, M.; Liu, R. Phenothiazine-Based Charge-Transfer Complexes as Visible-Light Photoinitiating Systems for Acrylate and Thiol-Ene Photopolymerization. *Prog. Org. Coat.* **2022**, *166*, 106772. [CrossRef]

125. Zhu, Y.; Xu, D.; Zhang, Y.; Zhou, Y.; Yagci, Y.; Liu, R. Phenacyl Phenothiazinium Salt as a New Broad-Wavelength-Absorbing Photoinitiator for Cationic and Free Radical Polymerizations. *Angew. Chem. Int. Ed.* **2021**, *60*, 16917–16921. [CrossRef]
126. Chao, P.; Gu, R.; Ma, X.; Wang, T.; Zhao, Y. Thiophene-Substituted Phenothiazine-Based Photosensitisers for Radical and Cationic Photopolymerization Reactions under Visible Laser Beams (405 and 455 Nm). *Polym. Chem.* **2016**, *7*, 5147–5156. [CrossRef]
127. Zhou, T.F.; Ma, X.Y.; Han, W.X.; Guo, X.P.; Gu, R.Q.; Yu, L.J.; Li, J.; Zhao, Y.M.; Wang, T. D–D–A Dyes with Phenothiazine–Carbazole/Triphenylamine as Double Donors in Photopolymerization under 455 Nm and 532 Nm Laser Beams. *Polym. Chem.* **2016**, *7*, 5039–5049. [CrossRef]
128. Wang, M.; Ma, X.; Yu, J.; Jia, X.; Han, D.; Zhou, T.; Yang, J.; Nie, J.; Wang, T. Aromatic Amine–Sulfone/Sulfoxide Conjugated D–π-A–π-D-Type Dyes in Photopolymerization under 405 Nm and 455 Nm Laser Beams. *Polym. Chem.* **2015**, *6*, 4424–4435. [CrossRef]
129. Hao, F.; Liu, Z.; Zhang, M.; Liu, J.; Zhang, S.; Wu, J.; Zhou, H.; Tian, Y. Four New Two-Photon Polymerization Initiators with Varying Donor and Conjugated Bridge: Synthesis and Two-Photon Activity. *Spectrochim. Acta. A. Mol. Biomol. Spectrosc.* **2014**, *118*, 538–542. [CrossRef]
130. Garra, P.; Dumur, F.; Gigmes, D.; Al Mousawi, A.; Morlet-Savary, F.; Dietlin, C.; Fouassier, J.P.; Lalevée, J. Copper (Photo)Redox Catalyst for Radical Photopolymerization in Shadowed Areas and Access to Thick and Filled Samples. *Macromolecules* **2017**, *50*, 3761–3771. [CrossRef]
131. Mousawi, A.A.; Kermagoret, A.; Versace, D.-L.; Toufaily, J.; Hamieh, T.; Graff, B.; Dumur, F.; Gigmes, D.; Fouassier, J.P.; Lalevée, J. Copper Photoredox Catalysts for Polymerization upon near UV or Visible Light: Structure/Reactivity/Efficiency Relationships and Use in LED Projector 3D Printing Resins. *Polym. Chem.* **2017**, *8*, 568–580. [CrossRef]
132. Xiao, P.; Dumur, F.; Zhang, J.; Fouassier, J.P.; Gigmes, D.; Lalevée, J. Copper Complexes in Radical Photoinitiating Systems: Applications to Free Radical and Cationic Polymerization upon Visible LEDs. *Macromolecules* **2014**, *47*, 3837–3844. [CrossRef]
133. Xiao, P.; Zhang, J.; Campolo, D.; Dumur, F.; Gigmes, D.; Fouassier, J.P.; Lalevée, J. Copper and Iron Complexes as Visible-Light-Sensitive Photoinitiators of Polymerization. *J. Polym. Sci. Part Polym. Chem.* **2015**, *53*, 2673–2684. [CrossRef]
134. Xiao, P.; Dumur, F.; Zhang, J.; Gigmes, D.; Fouassier, J.P.; Lalevée, J. Copper Complexes: The Effect of Ligands on Their Photoinitiation Efficiencies in Radical Polymerization Reactions under Visible Light. *Polym. Chem.* **2014**, *5*, 6350–6357. [CrossRef]
135. Dumur, F.; Bertin, D.; Gigmes, D. Iridium (III) Complexes as Promising Emitters for Solid–State Light–Emitting Electrochemical Cells (LECs). *Int. J. Nanotechnol.* **2012**, *9*, 377–395. [CrossRef]
136. Dumur, F.; Nasr, G.; Wantz, G.; Mayer, C.R.; Dumas, E.; Guerlin, A.; Miomandre, F.; Clavier, G.; Bertin, D.; Gigmes, D. Cationic Iridium Complex for the Design of Soft Salt-Based Phosphorescent OLEDs and Color-Tunable Light-Emitting Electrochemical Cells. *Org. Electron.* **2011**, *12*, 1683–1694. [CrossRef]
137. Tehfe, M.-A.; Lepeltier, M.; Dumur, F.; Gigmes, D.; Fouassier, J.-P.; Lalevée, J. Structural Effects in the Iridium Complex Series: Photoredox Catalysis and Photoinitiation of Polymerization Reactions under Visible Lights. *Macromol. Chem. Phys.* **2017**, *218*, 1700192. [CrossRef]
138. Telitel, S.; Dumur, F.; Telitel, S.; Soppera, O.; Lepeltier, M.; Guillaneuf, Y.; Poly, J.; Morlet-Savary, F.; Fioux, P.; Fouassier, J.-P.; et al. Photoredox Catalysis Using a New Iridium Complex as an Efficient Toolbox for Radical, Cationic and Controlled Polymerizations under Soft Blue to Green Lights. *Polym. Chem.* **2014**, *6*, 613–624. [CrossRef]
139. Lalevée, J.; Tehfe, M.-A.; Dumur, F.; Gigmes, D.; Blanchard, N.; Morlet-Savary, F.; Fouassier, J.P. Iridium Photocatalysts in Free Radical Photopolymerization under Visible Lights. *ACS Macro Lett.* **2012**, *1*, 286–290. [CrossRef]
140. Tang, Z.; Gao, Y.; Jiang, S.; Nie, J.; Sun, F. Cinnamoylformate Derivatives Photoinitiators with Excellent Photobleaching Ability and Cytocompatibility for Visible LED Photopolymerization. *Prog. Org. Coat.* **2022**, *170*, 106969. [CrossRef]
141. He, X.; Jia, W.; Gao, Y.; Jiang, S.; Nie, J.; Sun, F. Water-Soluble Benzoylformic Acid Photoinitiators for Water-Based LED-Triggered Deep-Layer Photopolymerization. *Eur. Polym. J.* **2022**, *167*, 111066. [CrossRef]
142. He, X.; Gao, Y.; Nie, J.; Sun, F. Methyl Benzoylformate Derivative Norrish Type I Photoinitiators for Deep-Layer Photocuring under Near-UV or Visible LED. *Macromolecules* **2021**, *54*, 3854–3864. [CrossRef]
143. Chen, H.; Noirbent, G.; Sun, K.; Brunel, D.; Gigmes, D.; Morlet-Savary, F.; Zhang, Y.; Liu, S.; Xiao, P.; Dumur, F.; et al. Photoinitiators Derived from Natural Product Scaffolds: Monochalcones in Three-Component Photoinitiating Systems and Their Applications in 3D Printing. *Polym. Chem.* **2020**, *11*, 4647–4659. [CrossRef]
144. Tang, L.; Nie, J.; Zhu, X. A High Performance Phenyl-Free LED Photoinitiator for Cationic or Hybrid Photopolymerization and Its Application in LED Cationic 3D Printing. *Polym. Chem.* **2020**, *11*, 2855–2863. [CrossRef]
145. Xu, Y.; Noirbent, G.; Brunel, D.; Ding, Z.; Gigmes, D.; Graff, B.; Xiao, P.; Dumur, F.; Lalevée, J. Allyloxy Ketones as Efficient Photoinitiators with High Migration Stability in Free Radical Polymerization and 3D Printing. *Dyes Pigments* **2021**, *185*, 108900. [CrossRef]
146. Xu, Y.; Ding, Z.; Zhu, H.; Graff, B.; Knopf, S.; Xiao, P.; Dumur, F.; Lalevée, J. Design of Ketone Derivatives as Highly Efficient Photoinitiators for Free Radical and Cationic Photopolymerizations and Application in 3D Printing of Composites. *J. Polym. Sci.* **2020**, *58*, 3432–3445. [CrossRef]
147. Chen, H.; Noirbent, G.; Liu, S.; Brunel, D.; Graff, B.; Gigmes, D.; Zhang, Y.; Sun, K.; Morlet-Savary, F.; Xiao, P.; et al. Bis-Chalcone Derivatives Derived from Natural Products as near-UV/Visible Light Sensitive Photoinitiators for 3D/4D Printing. *Mater. Chem. Front.* **2021**, *5*, 901–916. [CrossRef]

148. Liu, S.; Zhang, Y.; Sun, K.; Graff, B.; Xiao, P.; Dumur, F.; Lalevée, J. Design of Photoinitiating Systems Based on the Chalcone-Anthracene Scaffold for LED Cationic Photopolymerization and Application in 3D Printing. *Eur. Polym. J.* **2021**, *147*, 110300. [CrossRef]
149. Giacoletto, N.; Dumur, F. Recent Advances in Bis-Chalcone-Based Photoinitiators of Polymerization: From Mechanistic Investigations to Applications. *Molecules* **2021**, *26*, 3192. [CrossRef]
150. Ibrahim-Ouali, M.; Dumur, F. Recent Advances on Chalcone-Based Photoinitiators of Polymerization. *Eur. Polym. J.* **2021**, *158*, 110688. [CrossRef]
151. Chen, H.; Noirbent, G.; Liu, S.; Zhang, Y.; Sun, K.; Morlet-Savary, F.; Gigmes, D.; Xiao, P.; Dumur, F.; Lalevée, J. In Situ Generation of Ag Nanoparticles during Photopolymerization by Using Newly Developed Dyes-Based Three-Component Photoinitiating Systems and the Related 3D Printing Applications and Their Shape Change Behavior. *J. Polym. Sci.* **2021**, *59*, 843–859. [CrossRef]
152. Chen, H.; Vahdati, M.; Xiao, P.; Dumur, F.; Lalevée, J. Water-Soluble Visible Light Sensitive Photoinitiating System Based on Charge Transfer Complexes for the 3D Printing of Hydrogels. *Polymers* **2021**, *13*, 3195. [CrossRef] [PubMed]
153. Tehfe, M.-A.; Dumur, F.; Xiao, P.; Delgove, M.; Graff, B.; Fouassier, J.-P.; Gigmes, D.; Lalevée, J. Chalcone Derivatives as Highly Versatile Photoinitiators for Radical, Cationic, Thiol–Ene and IPN Polymerization Reactions upon Exposure to Visible Light. *Polym. Chem.* **2014**, *5*, 382–390. [CrossRef]
154. Sun, K.; Xu, Y.; Dumur, F.; Morlet-Savary, F.; Chen, H.; Dietlin, C.; Graff, B.; Lalevée, J.; Xiao, P. In Silico Rational Design by Molecular Modeling of New Ketones as Photoinitiators in Three-Component Photoinitiating Systems: Application in 3D Printing. *Polym. Chem.* **2020**, *11*, 2230–2242. [CrossRef]
155. Chen, H.; Regeard, C.; Salmi, H.; Morlet-Savary, F.; Giacoletto, N.; Nechab, M.; Xiao, P.; Dumur, F.; Lalevée, J. Interpenetrating Polymer Network Hydrogels Using Natural Based Dyes Initiating Systems: Antibacterial Activity and 3D/4D Performance. *Eur. Polym. J.* **2022**, *166*, 111042. [CrossRef]
156. Li, J.; Zheng, H.; Lu, H.; Li, J.; Yao, L.; Wang, Y.; Zhou, X.; Nie, J.; Zhu, X.; Fu, Z. Study on Pyrrole Chalcone Derivatives Used for Blue LED Free Radical Photopolymerization: Controllable Initiating Activity Achieved through Photoisomerization Property. *Eur. Polym. J.* **2022**, *176*, 111393. [CrossRef]
157. Allegrezza, M.L.; DeMartini, Z.M.; Kloster, A.J.; Digby, Z.A.; Konkolewicz, D. Visible and Sunlight Driven RAFT Photopolymerization Accelerated by Amines: Kinetics and Mechanism. *Polym. Chem.* **2016**, *7*, 6626–6636. [CrossRef]
158. Ciftci, M.; Tasdelen, M.A.; Yagci, Y. Sunlight Induced Atom Transfer Radical Polymerization by Using Dimanganese Decacarbonyl. *Polym. Chem.* **2014**, *5*, 600–606. [CrossRef]
159. Decker, C.; Bendaikha, T. Interpenetrating Polymer Networks. II. Sunlight-Induced Polymerization of Multifunctional Acrylates. *J. Appl. Polym. Sci.* **1998**, *70*, 2269–2282. [CrossRef]
160. Konkolewicz, D.; Schröder, K.; Buback, J.; Bernhard, S.; Matyjaszewski, K. Visible Light and Sunlight Photoinduced ATRP with Ppm of Cu Catalyst. *ACS Macro Lett.* **2012**, *1*, 1219–1223. [CrossRef]
161. Lalevée, J.; Fouassier, J.P. Recent Advances in Sunlight Induced Polymerization: Role of New Photoinitiating Systems Based on the Silyl Radical Chemistry. *Polym. Chem.* **2011**, *2*, 1107–1113. [CrossRef]
162. Li, J.; Lu, H.; Zheng, H.; Zhou, X.; Nie, J.; Zhu, X. Thermally Activated Pyrrole Chalcone Free Radical Photoinitiator with Excellent Stability to Sunlight. *Eur. Polym. J.* **2022**, *162*, 110884. [CrossRef]
163. Li, J.; Lu, H.; Zheng, H.; Li, J.; Yao, L.; Wang, Y.; Zhou, X.; Fu, Z.; Nie, J.; Zhu, X. Improvement in the Storage Stability of Free Radical Photocurable Materials under Sunlight Based on the Cis → Trans Photoisomerization of Pyrrole Chalcone Photoinitiator. *Prog. Org. Coat.* **2022**, *171*, 107025. [CrossRef]
164. Tehfe, M.-A.; Lalevée, J.; Gigmes, D.; Fouassier, J.P. Green Chemistry: Sunlight-Induced Cationic Polymerization of Renewable Epoxy Monomers Under Air. *Macromolecules* **2010**, *43*, 1364–1370. [CrossRef]
165. Wang, J.; Rivero, M.; Muñoz Bonilla, A.; Sanchez-Marcos, J.; Xue, W.; Chen, G.; Zhang, W.; Zhu, X. Natural RAFT Polymerization: Recyclable-Catalyst-Aided, Opened-to-Air, and Sunlight-Photolyzed RAFT Polymerizations. *ACS Macro Lett.* **2016**, *5*, 1278–1282. [CrossRef] [PubMed]
166. Yu, J.; Gao, Y.; Jiang, S.; Sun, F. Naphthalimide Aryl Sulfide Derivative Norrish Type I Photoinitiators with Excellent Stability to Sunlight under Near-UV LED. *Macromolecules* **2019**, *52*, 1707–1717. [CrossRef]
167. Li, J.; Zhang, X.; Nie, J.; Zhu, X. Visible Light and Water-Soluble Photoinitiating System Based on the Charge Transfer Complex for Free Radical Photopolymerization. *J. Photochem. Photobiol. Chem.* **2020**, *402*, 112803. [CrossRef]
168. Allen, N.S.; Chen, W.; Catalina, F.; Green, P.N.; Green, A. Photochemistry of Novel Water-Soluble Para-Substituted Benzophenone Photoinitiators: A Polymerization, Spectroscopic and Flash Photolysis Study. *J. Photochem. Photobiol. Chem.* **1988**, *44*, 349–360. [CrossRef]
169. Alupei, I.C.; Alupei, V.; Ritter, H. Cyclodextrins in Polymer Synthesis: Photoinitiated Free-Radical Polymerization of N-Isopropylacrylamide in Water Initiated by a Methylated β-Cyclodextrin/2-Hydroxy-2-Methyl-1-Phenylpropan-1-One Host/Guest Complex. *Macromol. Rapid Commun.* **2002**, *23*, 55–58. [CrossRef]
170. Balta, D.K.; Temel, G.; Aydin, M.; Arsu, N. Thioxanthone Based Water-Soluble Photoinitiators for Acrylamide Photopolymerization. *Eur. Polym. J.* **2010**, *46*, 1374–1379. [CrossRef]
171. Benedikt, S.; Wang, J.; Markovic, M.; Moszner, N.; Dietliker, K.; Ovsianikov, A.; Grützmacher, H.; Liska, R. Highly Efficient Water-Soluble Visible Light Photoinitiators. *J. Polym. Sci. Part Polym. Chem.* **2016**, *54*, 473–479. [CrossRef]

172. Bibaut-Renauld, C.; Burget, D.; Fouassier, J.P.; Varelas, C.G.; Thomatos, J.; Tsagaropoulos, G.; Ryrfors, L.O.; Karlsson, O.J. Use of α-Diketones as Visible Photoinitiators for the Photocrosslinking of Waterborne Latex Paints. *J. Polym. Sci. Part Polym. Chem.* **2002**, *40*, 3171–3181. [CrossRef]
173. Guo, L.; Yang, D.; Xia, L.; Qu, F.; Dou, Y.; Qu, F.; Kong, R.; You, J. A Highly Water-Soluble, Sensitive, Coumarin-Based Fluorescent Probe for Detecting Thiols, and Its Application in Bioimaging. *New J. Chem.* **2017**, *41*, 15277–15282. [CrossRef]
174. Eren, T.N.; Lalevée, J.; Avci, D. Bisphosphonic Acid-Functionalized Water-Soluble Photoinitiators. *Macromol. Chem. Phys.* **2019**, *220*, 1900268. [CrossRef]
175. Eren, T.N.; Lalevée, J.; Avci, D. Water Soluble Polymeric Photoinitiator for Dual-Curing of Acrylates and Methacrylates. *J. Photochem. Photobiol. Chem.* **2020**, *389*, 112288. [CrossRef]
176. Dietliker, K. Chapter 13 Water-Soluble Photoinitiators: Present and Future. In *Photopolymerisation Initiating Systems*; The Royal Society of Chemistry: London, UK, 2018; pp. 358–430. ISBN 978-1-78262-962-7.
177. Huang, X.; Wang, X.; Zhao, Y. Study on a Series of Water-Soluble Photoinitiators for Fabrication of 3D Hydrogels by Two-Photon Polymerization. *Dyes Pigments* **2017**, *141*, 413–419. [CrossRef]
178. Li, Z.; Torgersen, J.; Ajami, A.; Mühleder, S.; Qin, X.; Husinsky, W.; Holnthoner, W.; Ovsianikov, A.; Stampfl, J.; Liska, R. Initiation Efficiency and Cytotoxicity of Novel Water-Soluble Two-Photon Photoinitiators for Direct 3D Microfabrication of Hydrogels. *RSC Adv.* **2013**, *3*, 15939–15946. [CrossRef]
179. Knaus, S.; Gruber, H.F. Photoinitiators with Functional Groups. III. Water-Soluble Photoinitiators Containing Carbohydrate Residues. *J. Polym. Sci. Part Polym. Chem.* **1995**, *33*, 929–939. [CrossRef]
180. Kminek, I.; Yagci, Y.; Schnabel, W. A Water-Soluble Poly(Methylphenylsilylene) Derivative as a Photoinitiator of Radical Polymerization of Hydrophilic Vinyl Monomers. *Polym. Bull.* **1992**, *29*, 277–282. [CrossRef]
181. Le, C.M.Q.; Petitory, T.; Wu, X.; Spangenberg, A.; Ortyl, J.; Galek, M.; Infante, L.; Thérien-Aubin, H.; Chemtob, A. Water-Soluble Photoinitiators from Dimethylamino-Substituted Monoacylphosphine Oxide for Hydrogel and Latex Preparation. *Macromol. Chem. Phys.* **2021**, *222*, 2100217. [CrossRef]
182. Akhigbe, J.; Luciano, M.; Zeller, M.; Brückner, C. Mono- and Bisquinoline-Annulated Porphyrins from Porphyrin β,B′-Dione Oximes. *J. Org. Chem.* **2015**, *80*, 499–511. [CrossRef]
183. Allonas, X.; Lalevée, J.; Fouassier, J.P.; Tachi, H.; Shirai, M.; Tsunooka, M. Triplet State of O-Acyloximes Studied by Time-Resolved Absorption Spectroscopy. *Chem. Lett.* **2004**, *29*, 1090–1091. [CrossRef]
184. Chen, S.; Jin, M.; Malval, J.-P.; Fu, J.; Morlet-Savary, F.; Pan, H.; Wan, D. Substituted Stilbene-Based Oxime Esters Used as Highly Reactive Wavelength-Dependent Photoinitiators for LED Photopolymerization. *Polym. Chem.* **2019**, *10*, 6609–6621. [CrossRef]
185. Fast, D.E.; Lauer, A.; Menzel, J.P.; Kelterer, A.-M.; Gescheidt, G.; Barner-Kowollik, C. Wavelength-Dependent Photochemistry of Oxime Ester Photoinitiators. *Macromolecules* **2017**, *50*, 1815–1823. [CrossRef]
186. Hu, P.; Qiu, W.; Naumov, S.; Scherzer, T.; Hu, Z.; Chen, Q.; Knolle, W.; Li, Z. Conjugated Bifunctional Carbazole-Based Oxime Esters: Efficient and Versatile Photoinitiators for 3D Printing under One- and Two-Photon Excitation. *ChemPhotoChem* **2020**, *4*, 224–232. [CrossRef]
187. Lee, W.J.; Kwak, H.S.; Lee, D.; Oh, C.; Yum, E.K.; An, Y.; Halls, M.D.; Lee, C.-W. Design and Synthesis of Novel Oxime Ester Photoinitiators Augmented by Automated Machine Learning. *Chem. Mater.* **2022**, *34*, 116–127. [CrossRef]
188. Ma, X.; Cao, D.; Fu, H.; You, J.; Gu, R.; Fan, B.; Nie, J.; Wang, T. Multicomponent Photoinitiating Systems Containing Arylamino Oxime Ester for Visible Light Photopolymerization. *Prog. Org. Coat.* **2019**, *135*, 517–524. [CrossRef]
189. Pang, Y.; Fan, S.; Wang, Q.; Oprych, D.; Feilen, A.; Reiner, K.; Keil, D.; Slominsky, Y.L.; Popov, S.; Zou, Y.; et al. NIR-Sensitized Activated Photoreaction between Cyanines and Oxime Esters: Free-Radical Photopolymerization. *Angew. Chem. Int. Ed.* **2020**, *59*, 11440–11447. [CrossRef]
190. Sameshima, K.; Kura, H.; Matsuoka, Y.; Sotome, H.; Miyasaka, H. Improvement of the Photopolymerization and Bottom-Curing Performance of Benzocarbazole Oxime Ester Photoinitiators with Red-Shifted Absorption. *Jpn. J. Appl. Phys.* **2022**, *61*, 035504. [CrossRef]
191. Qiu, W.; Li, M.; Yang, Y.; Li, Z.; Dietliker, K. Cleavable Coumarin-Based Oxime Esters with Terminal Heterocyclic Moieties: Photobleachable Initiators for Deep Photocuring under Visible LED Light Irradiation. *Polym. Chem.* **2020**, *11*, 1356–1363. [CrossRef]
192. Breloy, L.; Negrell, C.; Mora, A.-S.; Li, W.S.J.; Brezová, V.; Caillol, S.; Versace, D.-L. Vanillin Derivative as Performing Type I Photoinitiator. *Eur. Polym. J.* **2020**, *132*, 109727. [CrossRef]
193. Allushi, A.; Kutahya, C.; Aydogan, C.; Kreutzer, J.; Yilmaz, G.; Yagci, Y. Conventional Type II Photoinitiators as Activators for Photoinduced Metal-Free Atom Transfer Radical Polymerization. *Polym. Chem.* **2017**, *8*, 1972–1977. [CrossRef]
194. Chen, Y.-C.; Kuo, Y.-T. Photocuring Kinetic Studies of TMPTMA Monomer by Type II Photoinitiators of Different Weight Ratios of 2-Chlorohexaaryl Biimidazole (o-Cl-HABI) and N-Phenylglycine (NPG). *J. Photopolym. Sci. Technol.* **2018**, *31*, 487–492. [CrossRef]
195. Li, J.; Zhang, X.; Ali, S.; Akram, M.Y.; Nie, J.; Zhu, X. The Effect of Polyethylene Glycoldiacrylate Complexation on Type II Photoinitiator and Promotion for Visible Light Initiation System. *J. Photochem. Photobiol. Chem.* **2019**, *384*, 112037. [CrossRef]
196. Kirschner, J.; Baralle, A.; Graff, B.; Becht, J.-M.; Klee, J.E.; Lalevée, J. 1-Aryl-2-(Triisopropylsilyl)Ethane-1,2-Diones: Toward a New Class of Visible Type I Photoinitiators for Free Radical Polymerization of Methacrylates. *Macromol. Rapid Commun.* **2019**, *40*, 1900319. [CrossRef]

197. Christmann, J.; Allonas, X.; Ley, C.; Ibrahim, A.; Croutxé-Barghorn, C. Triazine-Based Type-II Photoinitiating System for Free Radical Photopolymerization: Mechanism, Efficiency, and Modeling. *Macromol. Chem. Phys.* **2017**, *218*, 1600597. [CrossRef]
198. Kreutzer, J.; Kaya, K.; Yagci, Y. Poly(Propylene Oxide)-Thioxanthone as One-Component Type II Polymeric Photoinitiator for Free Radical Polymerization with Low Migration Behavior. *Eur. Polym. J.* **2017**, *95*, 71–81. [CrossRef]
199. Kabatc, J.; Iwińska, K.; Balcerak, A.; Kwiatkowska, D.; Skotnicka, A.; Czech, Z.; Bartkowiak, M. Onium Salts Improve the Kinetics of Photopolymerization of Acrylate Activated with Visible Light. *RSC Adv.* **2020**, *10*, 24817–24829. [CrossRef]
200. Kocaarslan, A.; Kütahya, C.; Keil, D.; Yagci, Y.; Strehmel, B. Near-IR and UV-LED Sensitized Photopolymerization with Onium Salts Comprising Anions of Different Nucleophilicities. *ChemPhotoChem* **2019**, *3*, 1127–1132. [CrossRef]
201. Fouassier, J.-P.; Morlet-Savary, F.; Lalevée, J.; Allonas, X.; Ley, C. Dyes as Photoinitiators or Photosensitizers of Polymerization Reactions. *Materials* **2010**, *3*, 5130–5142. [CrossRef]
202. Kabatc, J.; Ortyl, J.; Kostrzewska, K. New Kinetic and Mechanistic Aspects of Photosensitization of Iodonium Salts in Photopolymerization of Acrylates. *RSC Adv.* **2017**, *7*, 41619–41629. [CrossRef]
203. Fujiwara, T.; Nomura, K.; Inagaki, A. Cu–Pd Dinuclear Complexes with Earth-Abundant Cu Photosensitizer: Synthesis and Photopolymerization. *Organometallics* **2020**, *39*, 2464–2469. [CrossRef]
204. Wang, J.; Mathias, L.J. A Polymerizable Photosensitizer and Its Photopolymerization Kinetics. *Polym. Int.* **2005**, *54*, 1537–1542. [CrossRef]
205. Aydogan, B.; Gunbas, G.E.; Durmus, A.; Toppare, L.; Yagci, Y. Highly Conjugated Thiophene Derivatives as New Visible Light Sensitive Photoinitiators for Cationic Polymerization. *Macromolecules* **2010**, *43*, 101–106. [CrossRef]
206. Aydogan, B.; Gundogan, A.S.; Ozturk, T.; Yagci, Y. A Dithienothiophene Derivative as a Long-Wavelength Photosensitizer for Onium Salt Photoinitiated Cationic Polymerization. *Macromolecules* **2008**, *41*, 3468–3471. [CrossRef]
207. Aydogan, B.; Gundogan, A.S.; Ozturk, T.; Yagci, Y. Polythiophene Derivatives by Step-Growth Polymerizationvia Photoinduced Electron Transfer Reactions. *Chem. Commun.* **2009**, *41*, 6300–6302. [CrossRef] [PubMed]
208. Aydogan, B.; Yagci, Y.; Toppare, L.; Jockusch, S.; Turro, N.J. Photoinduced Electron Transfer Reactions of Highly Conjugated Thiophenes for Initiation of Cationic Polymerization and Conjugated Polymer Formation. *Macromolecules* **2012**, *45*, 7829–7834. [CrossRef]
209. Beyazit, S.; Aydogan, B.; Osken, I.; Ozturk, T.; Yagci, Y. Long Wavelength Photoinitiated Free Radical Polymerization Using Conjugated Thiophene Derivatives in the Presence of Onium Salts. *Polym. Chem.* **2011**, *2*, 1185–1189. [CrossRef]
210. Dumur, F. Recent Advances on Visible Light Thiophene-Based Photoinitiators of Polymerization. *Eur. Polym. J.* **2022**, *169*, 111120. [CrossRef]
211. Alizadeh, M.; Jalal, M.; Hamed, K.; Saber, A.; Kheirouri, S.; Tabrizi, F.P.F.; Kamari, N. Recent Updates on Anti-Inflammatory and Antimicrobial Effects of Furan Natural Derivatives. *J. Inflamm. Res.* **2020**, *13*, 451–463. [CrossRef]
212. Zheng, B.; Huo, L. Recent Advances of Furan and Its Derivatives Based Semiconductor Materials for Organic Photovoltaics. *Small Methods* **2021**, *5*, 2100493. [CrossRef]
213. Gidron, O.; Dadvand, A.; Wei-Hsin Sun, E.; Chung, I.; Shimon, L.J.W.; Bendikov, M.; Perepichka, D.F. Oligofuran-Containing Molecules for Organic Electronics. *J. Mater. Chem. C* **2013**, *1*, 4358–4367. [CrossRef]
214. Hendsbee, A.D.; Sun, J.-P.; McCormick, T.M.; Hill, I.G.; Welch, G.C. Unusual Loss of Electron Mobility upon Furan for Thiophene Substitution in a Molecular Semiconductor. *Org. Electron.* **2015**, *18*, 118–125. [CrossRef]
215. Mulay, S.V.; Bogoslavky, B.; Galanti, I.; Galun, E.; Gidron, O. Bifuran-Imide: A Stable Furan Building Unit for Organic Electronics. *J. Mater. Chem. C* **2018**, *6*, 11951–11955. [CrossRef]
216. Zhao, Z.; Nie, H.; Ge, C.; Cai, Y.; Xiong, Y.; Qi, J.; Wu, W.; Kwok, R.T.K.; Gao, X.; Qin, A.; et al. Furan Is Superior to Thiophene: A Furan-Cored AIEgen with Remarkable Chromism and OLED Performance. *Adv. Sci.* **2017**, *4*, 1700005. [CrossRef]
217. Wheeler, D.; Tannir, S.; Smith, E.; Tomlinson, A.; Jeffries-EL, M. A Computational and Experimental Investigation of Deep-Blue Light-Emitting Tetraaryl-Benzobis[1,2-d:4,5-D′]Oxazoles. *Mater. Adv.* **2022**, *3*, 3842–3852. [CrossRef]
218. Yoon, J.; Kim, S.K.; Kim, H.J.; Choi, S.; Jung, S.W.; Lee, H.; Kim, J.Y.; Yoon, D.-W.; Han, C.W.; Chae, W.-S.; et al. Asymmetric Host Molecule Bearing Pyridine Core for Highly Efficient Blue Thermally Activated Delayed Fluorescence OLEDs. *Chem.–Eur. J.* **2020**, *26*, 16383–16391. [CrossRef]
219. Bakhiya, N.; Appel, K.E. Toxicity and Carcinogenicity of Furan in Human Diet. *Arch. Toxicol.* **2010**, *84*, 563–578. [CrossRef]
220. EFSA Panel on Contaminants in the Food Chain (CONTAM); Knutsen, H.K.; Alexander, J.; Barregård, L.; Bignami, M.; Brüschweiler, B.; Ceccatelli, S.; Cottrill, B.; Dinovi, M.; Edler, L.; et al. Risks for Public Health Related to the Presence of Furan and Methylfurans in Food. *EFSA J.* **2017**, *15*, e05005. [CrossRef]
221. Li, J.; Hao, Y.; Zhong, M.; Tang, L.; Nie, J.; Zhu, X. Synthesis of Furan Derivative as LED Light Photoinitiator: One-Pot, Low Usage, Photobleaching for Light Color 3D Printing. *Dyes Pigments* **2019**, *165*, 467–473. [CrossRef]
222. Dumur, F. Recent Advances on Photobleachable Visible Light Photoinitiators of Polymerization. *Eur. Polym. J.* **2023**, *186*, 111874. [CrossRef]
223. Duan, C.; Adam, V.; Byrdin, M.; Ridard, J.; Kieffer-Jaquinod, S.; Morlot, C.; Arcizet, D.; Demachy, I.; Bourgeois, D. Structural Evidence for a Two-Regime Photobleaching Mechanism in a Reversibly Switchable Fluorescent Protein. *J. Am. Chem. Soc.* **2013**, *135*, 15841–15850. [CrossRef] [PubMed]

224. Guo, X.; Mao, H.; Bao, C.; Wan, D.; Jin, M. Fused Carbazole–Coumarin–Ketone Dyes: High Performance and Photobleachable Photoinitiators in Free Radical Photopolymerization for Deep Photocuring under Visible LED Light Irradiation. *Polym. Chem.* **2022**, *13*, 3367–3376. [CrossRef]
225. Li, Z.; Zou, X.; Zhu, G.; Liu, X.; Liu, R. Coumarin-Based Oxime Esters: Photobleachable and Versatile Unimolecular Initiators for Acrylate and Thiol-Based Click Photopolymerization under Visible Light-Emitting Diode Light Irradiation. *ACS Appl. Mater. Interfaces* **2018**, *10*, 16113–16123. [CrossRef]
226. Liao, W.; Xu, C.; Wu, X.; Liao, Q.; Xiong, Y.; Li, Z.; Tang, H. Photobleachable Cinnamoyl Dyes for Radical Visible Photoinitiators. *Dyes Pigments* **2020**, *178*, 108350. [CrossRef]
227. Liao, W.; Liao, Q.; Xiong, Y.; Li, Z.; Tang, H. Design, Synthesis and Properties of Carbazole-Indenedione Based Photobleachable Photoinitiators for Photopolymerization. *J. Photochem. Photobiol. Chem.* **2023**, *435*, 114297. [CrossRef]
228. Mitterbauer, M.; Knaack, P.; Naumov, S.; Markovic, M.; Ovsianikov, A.; Moszner, N.; Liska, R. Acylstannanes: Cleavable and Highly Reactive Photoinitiators for Radical Photopolymerization at Wavelengths above 500 Nm with Excellent Photobleaching Behavior. *Angew. Chem. Int. Ed.* **2018**, *57*, 12146–12150. [CrossRef]
229. Nan, X.; Huang, Y.; Fan, Q.; Shao, J.; Yao, Y. Different Photoinitiating Ability and Photobleaching Efficiency of Erythrosine B Derivatives in Radical/Cationic Photopolymerization. *Fibers Polym.* **2017**, *18*, 1644–1651. [CrossRef]
230. Rothman, J.H.; Still, W.C. A New Generation of Fluorescent Chemosensors Demonstrate Improved Analyte Detection Sensitivity and Photobleaching Resistance. *Bioorg. Med. Chem. Lett.* **1999**, *9*, 509–512. [CrossRef]
231. Takemura, F. Dye-Sensitized Photopolymerization of Vinyl Monomers. II. Photo-Bleaching of Acridine Yellow in Some Vinyl Monomers. *Bull. Chem. Soc. Jpn.* **1962**, *35*, 1078–1086. [CrossRef]
232. Terrones, G.; Pearlstein, A.J. Effects of Optical Attenuation and Consumption of a Photobleaching Initiator on Local Initiation Rates in Photopolymerizations. *Macromolecules* **2001**, *34*, 3195–3204. [CrossRef]
233. Wu, X.; Gong, S.; Chen, Z.; Hou, J.; Liao, Q.; Xiong, Y.; Li, Z.; Tang, H. Photobleachable Bis-Chalcones-Based Oxime Ester Dyes for Radical Visible Photopolymerization. *Dyes Pigments* **2022**, *205*, 110556. [CrossRef]
234. Xu, Y.; Noirbent, G.; Brunel, D.; Liu, F.; Gigmes, D.; Sun, K.; Zhang, Y.; Liu, S.; Morlet-Savary, F.; Xiao, P.; et al. Ketone Derivatives as Photoinitiators for Both Radical and Cationic Photopolymerizations under Visible LED and Application in 3D Printing. *Eur. Polym. J.* **2020**, *132*, 109737. [CrossRef]
235. Encinas, M.V.; Rufs, A.M.; Bertolotti, S.G.; Previtali, C.M. Xanthene Dyes/Amine as Photoinitiators of Radical Polymerization: A Comparative and Photochemical Study in Aqueous Medium. *Polymer* **2009**, *50*, 2762–2767. [CrossRef]
236. Garra, P.; Graff, B.; Morlet-Savary, F.; Dietlin, C.; Becht, J.-M.; Fouassier, J.-P.; Lalevée, J. Charge Transfer Complexes as Pan-Scaled Photoinitiating Systems: From 50 Mm 3D Printed Polymers at 405 Nm to Extremely Deep Photopolymerization (31 Cm). *Macromolecules* **2018**, *51*, 57–70. [CrossRef]
237. Garra, P.; Fouassier, J.P.; Lakhdar, S.; Yagci, Y.; Lalevée, J. Visible Light Photoinitiating Systems by Charge Transfer Complexes: Photochemistry without Dyes. *Prog. Polym. Sci.* **2020**, *107*, 101277. [CrossRef]
238. Lenka, S.; Nayak, P.L.; Ray, S. Photopolymerization Initiated by Charge-Transfer Complex: V—Photopolymerization of Methyl Methacrylate with the Use of Isoquinoline-Bromine Charge-Transfer Complex. *Polym. Photochem.* **1984**, *4*, 167–177. [CrossRef]
239. Mishra, M.K.; Lenka, S.; Nayak, P.L. Photopolymerization Initiated by Charge-Transfer Complex. I. Photopolymerization of Methylmethacrylate with the Use of Quinaldine-Bromine and Lutidine–Bromine Charge-Transfer Complexes as Photoinitiator. *J. Polym. Sci. Polym. Chem. Ed.* **1981**, *19*, 2457–2464. [CrossRef]
240. Derevyanko, D.I.; Shelkovnikov, V.V.; Kovalskii, V.Y.; Zilberberg, I.L.; Aliev, S.I.; Orlova, N.A.; Ugozhaev, V.D. The Charge Transfer Complex Formed between the Components of Photopolymer Material as an Internal Sensitizer of Spectral Sensitivity. *ChemistrySelect* **2020**, *5*, 11939–11947. [CrossRef]
241. Lenka, S.; Nayak, P.L.; Nayak, S.K. Photopolymerization Initiated by Charge-Transfer Complex. VII. Photopolymerization of Methyl Methacrylate with the Use of α-Picoline Chlorine Charge=Transfer Complex. *J. Macromol. Sci. Part-Chem.* **1983**, *20*, 835–845. [CrossRef]
242. Kurihara, T.; Sato, R.; Takeishi, M. Photopolymerization of Methyl Methacrylate in the Presence of a Charge-Transfer Complex of an Ether with Oxygen. *Polym. J.* **1991**, *23*, 1397–1400. [CrossRef]
243. Sakai, S.; Takahashi, K.; Sakota, N. Photopolymerization of Methyl Methacrylate Initiated by Iodine—Monoethanolamine. *Polym. J.* **1974**, *6*, 341–347. [CrossRef]
244. Kaya, K.; Kreutzer, J.; Yagci, Y. A Charge-Transfer Complex of Thioxanthonephenacyl Sulfonium Salt as a Visible-Light Photoinitiator for Free Radical and Cationic Polymerizations. *ChemPhotoChem* **2019**, *3*, 1187–1192. [CrossRef]
245. Wang, D.; Garra, P.; Lakhdar, S.; Graff, B.; Fouassier, J.P.; Mokbel, H.; Abdallah, M.; Lalevée, J. Charge Transfer Complexes as Dual Thermal and Photochemical Polymerization Initiators for 3D Printing and Composites Synthesis. *ACS Appl. Polym. Mater.* **2019**, *1*, 561–570. [CrossRef]
246. Wang, D.; Kaya, K.; Garra, P.; Fouassier, J.-P.; Graff, B.; Yagci, Y.; Lalevée, J. Sulfonium Salt Based Charge Transfer Complexes as Dual Thermal and Photochemical Polymerization Initiators for Composites and 3D Printing. *Polym. Chem.* **2019**, *10*, 4690–4698. [CrossRef]
247. Tasdelen, M.A.; Lalevée, J.; Yagci, Y. Photoinduced Free Radical Promoted Cationic Polymerization 40 Years after Its Discovery. *Polym. Chem.* **2020**, *11*, 1111–1121. [CrossRef]

248. Garra, P.; Caron, A.; Al Mousawi, A.; Graff, B.; Morlet-Savary, F.; Dietlin, C.; Yagci, Y.; Fouassier, J.-P.; Lalevée, J. Photochemical, Thermal Free Radical, and Cationic Polymerizations Promoted by Charge Transfer Complexes: Simple Strategy for the Fabrication of Thick Composites. *Macromolecules* **2018**, *51*, 7872–7880. [CrossRef]
249. Zhang, J.; Xiao, P. 3D Printing of Photopolymers. *Polym. Chem.* **2018**, *9*, 1530–1540. [CrossRef]
250. Tazuke, S. Initiation of Photopolymerization by Charge Transfer Interactions. *Pure Appl. Chem.* **1973**, *34*, 329–352. [CrossRef]
251. Perdana, F.; Eryanti, Y.; Zamri, A. Synthesis and Toxicity Assessments Some Para-Methoxy Chalcones Derivatives. *Int. Symp. Appl. Chem. 2015* **2015**, *16*, 129–133. [CrossRef]
252. Salehi, B.; Quispe, C.; Chamkhi, I.; El Omari, N.; Balahbib, A.; Sharifi-Rad, J.; Bouyahya, A.; Akram, M.; Iqbal, M.; Docea, A.O.; et al. Pharmacological Properties of Chalcones: A Review of Preclinical Including Molecular Mechanisms and Clinical Evidence. *Front. Pharmacol.* **2021**, *11*, 592654. [CrossRef]
253. Elkanzi, N.A.A.; Hrichi, H.; Alolayan, R.A.; Derafa, W.; Zahou, F.M.; Bakr, R.B. Synthesis of Chalcones Derivatives and Their Biological Activities: A Review. *ACS Omega* **2022**, *7*, 27769–27786. [CrossRef] [PubMed]
254. Tekale, S.; Mashele, S.; Pooe, O.; Thore, S.; Kendrekar, P. Rajandra Pawar Biological Role of Chalcones in Medicinal Chemistry. In *Vector-Borne Diseases*; Claborn, D., Bhattacharya, S., Roy, S., Eds.; IntechOpen: Rijeka, Croatia, 2020; p. 9. ISBN 978-1-83880-022-2.
255. Rozmer, Z.; Perjési, P. Naturally Occurring Chalcones and Their Biological Activities. *Phytochem. Rev.* **2016**, *15*, 87–120. [CrossRef]
256. Gou, L.; Opheim, B.; Coretsopoulos, C.N.; Scranton, A.B. Consumption of the Molecular Oxygen in Polymerization Systems Using Photosensitized Oxidation of Dimethylanthracene. *Chem. Eng. Commun.* **2006**, *193*, 620–627. [CrossRef]
257. Sanai, Y.; Kagami, S.; Kubota, K. Initiation and Termination Pathways in the Photopolymerization of Acrylate Using Methyl Phenylglyoxylate as an Initiator. *Polym. J.* **2020**, *52*, 375–385. [CrossRef]
258. Hu, S.; Wu, X.; Neckers, D.C. Methyl Phenylglyoxylate as a Photoinitiator. *Macromolecules* **2000**, *33*, 4030–4033. [CrossRef]
259. Hu, S.; Popielarz, R.; Neckers, D.C. Fluorescence Probe Techniques (FPT) for Measuring the Relative Efficiencies of Free-Radical Photoinitiators. *Macromolecules* **1998**, *31*, 4107–4113. [CrossRef]
260. Topa, M.; Ortyl, J. Moving Towards a Finer Way of Light-Cured Resin-Based Restorative Dental Materials: Recent Advances in Photoinitiating Systems Based on Iodonium Salts. *Materials* **2020**, *13*, 4093. [CrossRef]
261. Rasaki, S.A.; Xiong, D.; Xiong, S.; Su, F.; Idrees, M.; Chen, Z. Photopolymerization-Based Additive Manufacturing of Ceramics: A Systematic Review. *J. Adv. Ceram.* **2021**, *10*, 442–471. [CrossRef]